Bol. Soc. Paran. Mat.
©SPM – E-ISSN-2175-1188
SPM: www.spm.uem.br/bspm

(3s.) **v. 2026 (44) 2** : 1–28.
ISSN-0037-8712
doi:10.5269/bspm.78055

Effect of Delay on Coral Reef Ecosystem with Disease Presence in Coral Species

Santosh Biswas [1], Buddhadev Ranjit [1], Saddam Mollah [2], Joydev Chattopadhyay [3], Subhas Khajanchi [4] and Bashir Ahmad [5] *

ABSTRACT: Taking into account the effect of incubation time delay, a coral reef system with disease present in coral species is studied in this paper. We present the qualitative analysis of the model including existence and positivity of its solutions. Local asymptotic stability of the biologically feasible equilibria in case of both delayed and non-delayed system is discussed. The Hopf-bifurcation analysis for the system around the interior equilibrium is also performed by treating time delay as a bifurcation parameter. We derive the direction of Hopf-bifurcation, the stability and period of bifurcating periodic solutions by applying the normal form theory and central manifold theorem. We perform numerical investigation and explore their biological implication to support our theoretical results. Our findings indicate that incubation delay is responsible for destabilizing the system and can generate a cycle. In addition, conversion rate of infected colonies to healthy coral can prevent the oscillation within the system, and controls disease transmission among coral species.

Key Words: Coral reef, disease, incubation delay, stability analysis, Hopf bifurcation, numerical investigations.

Contents

1. Introduction

Coral is an undersea organism, and each individual coral is known as a polyp. Thousands of identical polyps live together and form a coral colony, which is known as reef building coral. As coral cannot produce food, it develops a mutualistic relationship with algae which resides inside the tissues of corals. A safe habitat for the algae and the material needed for photosynthesis are provided by the coral. Algae help the coral by producing oxygen and removing waste while the coral helps algae in maintaining theirs environment. Coral reefs play an important role in the marine ecosystem by providing habitat and source of food for several marine species [1].

Among other productive and biologically diverse ecosystems, reefs are the most diverse in nature on the earth [2]. and provide at least 500 million people in 109 different nations with life-saving medicines and services, coastal protection, as well as tourism and cultural benefits [3,4]. Researchers have speculated that approximately (0.1-0.5)% of the sea floor is covered by coral reefs [3,5]. These reefs provide food and habitat for roughly one third of the world's marine fish species [6]. In addition, coral reefs are globally

* Corresponding author.
2020 *Mathematics Subject Classification:* 92B05, 92D25, 34C23.
Submitted July 24, 2025. Published January 21, 2026

present along the shores of more than 100 countries and territories. A large number of people in these countries relies on coral reefs for food or protein [7].

Unfortunately, coral reefs are under severe threat due to biotic (pathogen, parasite, etc.) and abiotic (change in salinity, temperature, light, etc.) factors which are causing worldwide coral decline [8,9]. Among the other factors, coral disease is one of the most significant causes of coral degeneration [10,11]. Coral disease is an abnormal condition of coral reefs. Although the mechanism of coral disease is not clear, scientists have identified important drivers of coral disease such as global warming [12] and other anthropogenic pressures like over harvesting of reef organisms, destructive fishing methods, uncontrolled tourism [13]. Experimental biologists are till now working on it and try to identify the pathogens associated with coral disease.

Coral is infected through direct contact (from infected to susceptible corals) and indirect contact (by pathogen) [14]. It releases toxins through their mesenteric filaments that infect the tissues of neighbouring colonies [14]. For example, parts of the black band disease (BBD) like microbial mat have been transferred from infected colonies to unaffected colonies within the same reef [14,15]. On the other hand, white band disease (WBD) is caused due to bacterial infections. Furthermore, corals are infected via pathogens, which happen in two ways namely, water-mediated and vector-mediated. Water-mediated transport is a key transmission route for spreading a number of coral diseases, including WBD, WPD, WPX, WS, PUWS, SEB and BBD, that can facilitate the movement of free-living pathogens. These pathogens or infectious agents originating from infected cells in coral reefs can potentially be transported over a large range of the oceans. It has been observed that some pathogens (e.g, ciliate Halofolliculina spp., a variety of Vibrio spp., etc.) have been chosen to colonise plastic marine debris [16,17] . These debris are then connected to a prevalence risk of coral disease [18]. It is imperative to note that water-borne transmission for WBD and SEB was only successful when corals were damaged prior to trial exposure [19,20]. There also exists another disease transmission mode of coral population through diverse organisms, which are also called coral predators or corallivores. Experimental studies demonstrate that disease also spreads from infected to susceptible corals via vectors such as corallivores reef fish [21] and crown-of-thorns starfish [22]. If a corallivore feeds on a disease tissue, mucus including the skeletons of living soft and hard corals [1,23] then feeds on a healthy coral, which may allow the infection to enter by another transmission pathway (water-borne transmission) due to ingest the pathogen [24]. So predators can act as disease vectors or as reservoirs for pathogens [25]. On the contrary, some others corallivores may decline disease occurrence. Thus both of them are positively [26] and negatively [27] associated with disease progression. Moreover, numerous studies indicate that disease transmission and progression rates are considerably correlated with vector and host densities [24,28,29], intensity of coral bleaching [28,30], poor water quality [31], sufficiently high seawater temperatures as well as UV radiation [32,33].

In the real world, the behavior of a biological system cannot be understood immediately. Instead, it depends on the past history of the system. It is well known that the time lag is a very common phenomenon in population biology. However, it is complicated biological process and needs to be addressed for practical purposes. In biological systems, time delay may arise due to numerous reasons namely, maturation [35,34], incubation delay due to infectious agent developing in the host [36,37,38], continuously distributed and discrete time delay for cancer-immune interaction [39,40], restoration of reef structure [41], etc. It is obvious that time lag plays an important role in the kinetics of cancer immune interaction system. Sardar et al [39] studied the impact of continuously distributed delay to address the interaction among tumor cells, tumor-specific CD8+T cells, helper T cells and IL-2 via a system of coupled nonlinear differential equations. Their study has revealed that the activation rate of CD8+T cells can prevent the oscillation of tumor-presence equilibria. In another work, Sardar et al [40] addressed a three dimensional model of cancer cells, immune effector cells and IL-2. They have also incorporated a discrete time lag between the recruitment of IL-2 due to cytotoxic-T-lymphocytes and the immune cell activation in presence of IL-2. Their theoretical and numerical analysis has shown that the effector cells can cause the tumor cell population to regress in presence of IL-2. Until now, there are a few works dealing with coral-algal interactions in coral reefs ecosystem in presence of time delay; for instance,

see [41,38]. Blackwood et al [41] incorporated a time delay into a model of coral-algal interactions in Caribbean coral reefs and their study revealed alternative stable states, namely a favorable coral-rich state and a degraded coral-depleted state. They also remarked the importance of comprehending not only the asymptotic behavior but also the basins of attraction for stable equilibria within the system. Bhattacharyya et al. [38] investigated the role of a discrete time lag on the recovery of algal turf following macroalgae grazing by herbivores. They also explored the effect of an incubation time lag for infectious agents to develop inside susceptible corals after contacting with infected corals. According to their findings, when the parameters representing time delays surpass a critical value, the stability of the interior equilibrium is lost, leading to a Hopf-bifurcation. As far as we know, the present work is the first attempt in the theoretical study of coral reef system with disease present in coral and incubation time delay. In this article, we modify the model studied by Briggs *et al.* [42] that captures the temporal nature of coral reef ecosystem by incorporating disease in reef ecosystem. Next, we incorporate the incubation time lag into the incident rate which follows law of mass action. The lag represents the time period in which the infectious agents develop in the healthy coral and the coral only makes itself infectious after that time.

The rest of the article is arranged as follows. In Section 2, we formulate the mathematical model by assuming certain hypotheses. we discuss the existence and positivity of solutions for the given model in Section 3. Section 4 deals with a qualitative analysis of the model without time lag, that is, we find the equilibria together with their feasibility, and local stability of the system. In presence of time lag, stability and existence of Hopf-bifurcation around an interior equilibrium point is investigated in Section 5. We determine the criteria for switching stability of the system with time lag, and the duration of time delay preserving the local stability. Applying the technique due to Hassard *et al.* [43], we obtain the direction, stability and period of Hopf-bifurcating periodic solution of the system. Section 6 is devoted to the numerical investigation for validation of our theoretical results. The paper concludes with some interesting observations.

2. Formulation of the Mathematical Model

We consider a model studied by Briggs *et al.* [42] that captures the temporal nature of coral reef ecosystem, where the space on a reef is inhabited by vital benthic organisms namely coral, macroalgae, and turf algae. This model has revealed that the dynamics of fraction of the space inhabited by these key groups changes over time. In the natural environment, these groups can exhibit a significant species diversity. However, for modelling of coral reef ecosystem, Briggs *et al.* [42] considered macroalgae as a single, unstructured, state variable (commonly used hypothesis), in which all life stages were equally vulnerable to herbivory. They also assumed that any vacant space on the reef was promptly filled by turf, refering to low-growing filamentous algae with a height of less than 10 mm. They classified crustose coralline algae as a part of the turf category for the reason that both turf and crustose coralline algae substrates could be overgrown by either coral or macroalgae. Herbivorous fish have the potential to control macroalgae, which are competitors of corals for space [44]. In their model, they did not explicitly account for the population dynamics of fish but incorporated the loss of algae caused by herbivory into the macroalgae mortality rate. The model [42] delineates the temporal dynamics of the fractions of benthic space on the reef ecosystem and is governed by a system of coupled nonlinear ordinary differential equations:

$$\begin{aligned} \frac{dC}{dt} &= rT + gTC - \gamma g_1 MC - dC \\ \frac{dM}{dt} &= \mu T + g_1 TM + \gamma g_1 MC - vM, \end{aligned} \tag{2.1}$$

where the space on the reef is inhabited by coral (C), macroalgae (M), and turf (T). At any time t, the entire reef space falls into one of these three states ($C(t),\ M(t),\ T(t)$) with $C(t) + M(t) + T(t) = 1$.

Following [42], we consider that both coral and macroalgae may be recruited either locally or from external sources/open recruitment. Open recruitment of propagules exclusively arises due to the free space available for corals as well as macroalgae. The lateral growth of coral is restricted to free space only, while macroalgae have the capability to grow over both free space and existing coral. The term $r(\mu)$ indicates the recruitment rate of coral (macroalgae) and g represents the rate at which free space is

occupied due to the combined effects of local recruitment of coral to free space and the lateral growth of coral over that free space. The term g_1TM describes the combined rate of local recruitment and lateral growth of macroalgae over free space. It is assume that the growth rate of macroalgae is typically slower over coral compared to free space. Consequently, the macroalgae growth rate over coral is γg_1 with a scaling parameter γ (≤ 1). The parameters d and v represent the death rates of coral and vulnerable macroalgae, respectively. In this model, all macroalgae are considered to be vulnerable and the model does not incorporate herbivorous fish as dynamic variables. So the grazing pressure on macroalgae by fish is incorporated into the macroalgae mortality rate (v). If the population of herbivorous fish is reduced due to fishing, the value of the parameter v will decrease accordingly.

It is well established from experimental studies [1,21,22,23,24,25] that disease spreads from infected to susceptible corals via vectors and may influence reef structure and dynamics. Black band disease (BBD) is spread from infected to susceptible corals via direct contact [38]. Williams et al. [45] and Vollmer et al. [46] point out that white band disease (WBD) spreads through coral-coral contact. Thus, the coral disease is one of the vital causes of coral degeneration. With this background, we modify the model proposed by Briggs *et al.* [42] by incorporating disease in coral reef. With the presence of disease in coral [47,10], our coral population model is derived from the classic disease models (SI models) which predict the dynamics of susceptible/healthy and infected individuals [48,49]. To simplify our model, we assume that the disease transmission occurs via a contagious pathway, where infected coral colonies (I) spread the disease to susceptible healthy coral colonies (S) through the release of pathogens into the water column. The disease transmission process obeys the mass-action principle as λSI, where the parameter λ represents the disease transmission rate and it roughly indicates the fraction of encounters leading to instantaneous infection. Infected coral colonies experience an additional mortality rate of e. Coral colonies have an ability to recover from lesions through tissue regeneration or by shedding diseased tissue, giving rise to no longer visible signs of infection [50]. Further, we assume that the recovered colonies remain susceptible to disease and the infected colonies come back to the susceptible class at instantaneous rate ω. Based on the aforementioned assumptions, the model (2.1) takes the form:

$$\begin{aligned} \frac{dS}{dt} &= rT + gT(S+I) - \gamma g_1 M(S+I) - dS - \lambda SI + \omega I \\ \frac{dI}{dt} &= \lambda SI - (d+e)I - \omega I \\ \frac{dM}{dt} &= \mu T + g_1 TM + \gamma g_1 M(S+I) - vM. \end{aligned} \tag{2.2}$$

It is well established that the time delay is a common and complicated phenomenon in population biology. The time delay between the two events, namely the first effective contact between healthy and infected individuals and the newly infected individual accounts for productive infectious. The lag (τ) represents the time period in which the infectious agents develop into the healthy coral to make it infectious. Thus, the time lag is introduced in the model (2.2) to have the following form

$$\begin{aligned} \frac{dS}{dt} &= rT + gT(S+I) - \gamma g_1 M(S+I) - dS - \lambda \int_{-\infty}^{t} S(\tilde{\kappa})I(\tilde{\kappa})\Pi(t-\tilde{\kappa})d\tilde{\kappa} + \omega I \\ \frac{dI}{dt} &= \lambda \int_{-\infty}^{t} S(\tilde{\kappa})I(\tilde{\kappa})\Pi(t-\tilde{\kappa})d\tilde{\kappa} - (d+e)I - \omega I \\ \frac{dM}{dt} &= \mu T + g_1 TM + \gamma g_1 M(S+I) - vM. \end{aligned} \tag{2.3}$$

The infected coral at time t is rising from the healthy coral at time $t-\tilde{\kappa}$ and the memory (or probability distribution) function of $\tilde{\kappa}$ is Π. This memory function is defined as follows:

$$\Pi = \frac{\sigma^{j+1}\tilde{\kappa}^j}{j!} exp(-\sigma\tilde{\kappa}),$$

where σ is a positive constant and $j \in \mathbb{Z}$ is known as the order of time lag. According to [51], the average time lag is determined as

$$\tilde{T} = \int_0^{\infty} \tilde{\kappa}\Pi(\tilde{\kappa})d\tilde{\kappa} = \frac{j+1}{\sigma}.$$

Now we consider the memory function in terms of the delta function as

$$\Pi = \delta(\tilde{\kappa} - \tau),$$

where τ is a non-negative constant. Thus, the model (2.3) becomes

$$\begin{array}{rcl} \frac{dS}{dt} & = & rT + gT(S+I) - \gamma g_1 M(S+I) - dS - \lambda S(t-\tau)I(t-\tau) + \omega I \\ \frac{dI}{dt} & = & \lambda S(t-\tau)I(t-\tau) - (d+e)I - \omega I \\ \frac{dM}{dt} & = & \mu T + g_1 TM + \gamma g_1 M(S+I) - vM. \end{array} \tag{2.4}$$

In this model, it is assumed that a particular region of the seabed is covered entirely by healthy coral (S), infected coral (I), macroalgae (M), and algal turfs (T), so that $S+I+M+T=1$. Thus, the model takes the form:

$$\begin{array}{rcl} \frac{dS}{dt} & = & \Big[r + g(S+I)\Big]\Big[1-(S+I+M)\Big] - \gamma g_1 M(S+I) - dS \\ & & -\lambda S(t-\tau)I(t-\tau) + \omega I \equiv F_1(S,I,M), \\ \frac{dI}{dt} & = & \lambda S(t-\tau)I(t-\tau) - (d+e)I - \omega I \equiv F_2(S,I,M), \\ \frac{dM}{dt} & = & \Big[\mu + g_1 M\Big]\Big[1-(S+I+M)\Big] + \gamma g_1 M(S+I) - vM \equiv F_3(S,I,M). \end{array} \tag{2.5}$$

The initial conditions equipped with the system (2.5) are given by

$$S(\phi) = \psi_1(\phi), I(\phi) = \psi_2(\phi), M(\phi) = \psi_3(\phi), -\tau \le \phi \le 0, \tag{2.6}$$

where $\psi = (\psi_1, \psi_2, \psi_3)^T \in \mathcal{C}_+$ such that $\psi_i(\phi) \ge 0, i = 1,2,3, \forall\ \phi \in [-\tau, 0]$ and $\mathcal{C}_+ = \mathcal{C}_+([-\tau,0], \mathbf{R}^3_{+0})$ is the Banach space endowed with the norm $\|\psi\| = \sup_{-\tau \le \phi \le 0}\{|\psi_1(\phi)|, |\psi_2(\phi)|, |\psi_3(\phi)|\}$ for ψ in $\mathcal{C}_+$.

Further, for the biological feasibility, it is assumed that $\psi_i(0) > 0$, for $i = 1,2,3$.

3. A Preliminary Result

Lemma 3.1 *(Existence and positive invariance) The system (2.5) with initial conditions (2.6) has a unique solution $(S(t), I(t), M(t))$ in the interval $[0, \infty)$ and remains positive $\forall\ t > 0$.*

Proof: Let us express the model (2.5) as $\dot{Z} = F(Z)$, where $Z \equiv (S, I, M)^T$ and $F : \mathcal{C}_+ \longrightarrow \mathbf{R^3_{+0}}$ with $F = (F_1, F_2, F_3)^T$, $F_i \in \mathcal{C}^\infty(\mathbf{R_{+0}}), i = 1,2,3$. Then, we have

$$\begin{aligned} F_1 &= \Big[r + g(S+I)\Big]\Big[1-(S+I+M)\Big] - \gamma g_1 M(S+I) - dS - \lambda S(t-\tau)I(t-\tau) + \omega I, \\ F_2 &= \lambda S(t-\tau)I(t-\tau) - (d+e)I - \omega I, \\ F_3 &= \Big[\mu + g_1 M\Big]\Big[1-(S+I+M)\Big] + \gamma g_1 M(S+I) - vM. \end{aligned}$$

Let $Z(\phi) = (\psi_1(\phi), \psi_2(\phi), \psi_3(\phi)) \in \mathcal{C}_+$ and $\psi_i(\phi) \ge 0$ for $i = 1,2,3$ with $\phi \in [-\tau, 0]$, $\tau > 0$. Since F is a locally Lipschitzian and completely continuous function of variables S, I, M in $\Omega = \{(S(t), I(t), M(t)); S > 0, I > 0, M > 0\}$, therefore, by the lemma [52], the system (2.5) with initial conditions (2.6) has a unique solution in the interval $[0, a_0]$, $\forall\ t \ge 0$, where a_0 is a finite positive real number. □

4. Qualitative Analysis of the System without Time Lag

The system (2.5) has two non-negative equilibria in absence of time lag ($\tau = 0$). Observe that $L_1(S_1, 0, M_1)$ is the disease free equilibrium, where $S_1 = \frac{\mu + (g_1 - v - \mu)M_1 - gM_1^2}{\mu + (1-\gamma)g_1 M_1}$ and M_1 is the positive zero of the polynomial equation

$$a_0 M_1^4 + a_1 M_1^3 + a_2 M_1^2 + a_3 M_1 + a_4 = 0, \tag{4.1}$$

with

$$\begin{aligned}
a_0 &= g^3 + g_1^3(1-\gamma)^2 - gg_1^2(1-\gamma),\\
a_1 &= 2\mu g_1^2(1-\gamma) - g^2 g_1(1-\gamma) - \mu g g_1 + g_1^2(1-\gamma)(g_1 - v - \mu) - \frac{dgg_1(1-\gamma)}{r+\mu+1} + \frac{vg_1^2(1-\gamma)^2}{r+\mu+1},\\
a_2 &= g(g_1 - v - \mu)^2 - 2g^2(g_1 - v - \mu) - 2\mu g^2 + g_1\mu^2 - g^2\mu + g_1(1-\gamma)(g_1 - v - \mu)\\
&+ \mu g_1(g_1 - v - \mu) + \mu g_1^2(1-\gamma) - \frac{gd\mu}{r+\mu+1} + \frac{dg_1(1-\gamma)(g_1 - v - \mu)}{r+\mu+1} + \frac{2v\mu g_1(1-\gamma)}{r+\mu+1}\\
&- \frac{(r+\mu)g_1^2(1-\gamma)^2}{r+\mu+1},\\
a_3 &= \mu g(g_1 - v - \mu) + \mu g g_1(1-\gamma) + g_1\mu^2 + \frac{d\{(g_1 - v - \mu)\mu + \mu g_1(1-\gamma)\}}{r+\mu+1} + \frac{v\mu^2}{r+\mu+1}\\
&- \frac{(r+\mu)2\mu g_1(1-\gamma)}{r+\mu+1},\\
a_4 &= 2g\mu^2 + 2\mu g(g_1 - v - \mu) + \frac{d\mu^2}{r+\mu+1} - \frac{(r+\mu)\mu^2}{r+\mu+1}.
\end{aligned}$$

The coexisting positive interior equilibrium point is $L_*(S_*, I_*, M_*)$, where $S_* = \frac{d+e+\omega}{\lambda}$ and $I_* = \frac{(\mu+g_1M_*)(1-S_*-M_*)+(\gamma g_1 S_* - v)M_*}{\mu+(1-\gamma)g_1M_*}$ with M_* being the positive root of the following equation

$$b_0M^5 + b_1M^4 + b_2M^3 + b_3M^2 + b_4M + b_5 = 0, \tag{4.2}$$

with

$$\begin{aligned}
b_0 &= rg_1^2,\\
b_1 &= -2g_1(-\mu + g_1 - g_1S_* + \gamma g_1 S_* - v)r,\\
b_2 &= r(-\mu + g_1 - g_1S_* + \gamma g_1 S_* - v)^2 - 2\mu g_1(1-S_*) - g_1\{2rS_* + (1+\gamma)g\} + (g - r - \lambda S_*\\
&+ \omega)g_1^2(1-\gamma),\\
b_3 &= 2r\mu(1-S_*)(-\mu + g_1 - g_1S_* + \gamma g_1 S_* - v) + \{2rS_* + (1+\gamma)g\}(-\mu + g_1 - g_1S_* + \gamma g_1 S_* - v)\\
&+ \{rS_*^2 + (1+\gamma)gS_*\}g_1(1-\gamma) - (g - r - \lambda S_* + \omega)\{g_1(1-\gamma)(-\mu + g_1 - g_1S_* + \gamma g_1 S_* - v\\
&- g_1\mu)\} - \{r + (g - r - d)S_*\}g_1^2(1-\gamma)^2,\\
b_4 &= r\mu^2(1-S_*)^2 + \{2rS_* + (1+\gamma)g\}\mu(1-S_*) + \{rS_*^2 + (1+\gamma)gS_*\}\mu - (g - r - \lambda S_* + \omega)\\
&\{\mu(-\mu + g_1 - g_1S_* + \gamma g_1 S_* - v) + g_1(1-\gamma)\mu(1-S_*)\} - \{r + (g - r - d)S_*\}2\mu g_1(1-\gamma),\\
b_5 &= -[(g - r - \lambda S_* + \omega)\mu^2(1-S_*) + \{r + (g - r - d)S_*\}\mu^2].
\end{aligned}$$

So the disease free equilibrium point $L_1(S_1, 0, M_1)$ is admissible for $g_1 > g_1^0$ with $g_1^0 = gM_1 + v + \mu(1 - \frac{1}{M_1})$ and the sufficient condition for existence of positive interior equilibrium point $L_*(S_*, I_*, M_*)$ is $S_* > \frac{v}{\gamma g_1}$.

4.1. Stability analysis

Here, we discuss the local stability of the system (2.5) around the disease free and interior equilibrium points. The Jacobian matrix at the disease free equilibrium point $L_1(S_1, 0, M_1)$ is

$$J_1 = \begin{bmatrix} \frac{\partial F_1}{\partial S}|_{(S_1,0,M_1)} & \frac{\partial F_1}{\partial I}|_{(S_1,0,M_1)} & \frac{\partial F_1}{\partial M}|_{(S_1,0,M_1)} \\ 0 & \frac{\partial F_2}{\partial I}|_{(S_1,0,M_1)} & 0 \\ \frac{\partial F_3}{\partial S}|_{(S_1,0,M_1)} & \frac{\partial F_3}{\partial I}|_{(S_1,0,M_1)} & \frac{\partial F_3}{\partial M}|_{(S_1,0,M_1)} \end{bmatrix}.$$

The characteristic values of the Jacobian matrix J_1 are $\lambda_1 = \frac{\partial F_2}{\partial I}|_{(S_1,0,M_1)} = \lambda S_1 - (d + e + \omega)$ and other two values are the zeros of the equation

$$\lambda^2 - \lambda \left(\frac{\partial F_1}{\partial S}|_{(S_1,0,M_1)} + \frac{\partial F_3}{\partial M}|_{(S_1,0,M_1)} \right) + \frac{\partial (F_1, F_3)}{\partial (S, M)}|_{(S_1,0,M_1)} = 0.$$

The zeros of the equation are negative or having negative real parts if $\frac{\partial F_1}{\partial S}|_{(S_1,0,M_1)} + \frac{\partial F_3}{\partial M}|_{(S_1,0,M_1)} < 0$ and $\frac{\partial (F_1,F_3)}{\partial (S,M)}|_{(S_1,0,M_1)} > 0$. Now the characteristic value $\lambda_1 = \frac{\partial F_2}{\partial I}|_{(S_1,0,M_1)} < 0$ when $R_0 < 1$, where the threshold parameter R_0 is defined by

$$R_0 = \left\{ \frac{\lambda S_1}{d + e + \omega} \right\} = \left\{ \frac{\text{Infection rate of a new infective coral}}{\text{Removal rate of infected coral}} \right\},$$

that is, the ratio between the infection rate of a new infective coral appearing in fully susceptible/healthy coral species and the removal rate of infected coral species around $L_1(S_1, 0, M_1)$. After some algebraic manipulation, we have $\frac{\partial F_1}{\partial S}|_{(S_1,0,M_1)} + \frac{\partial F_3}{\partial M}|_{(S_1,0,M_1)} < 0$ when $r > r_{[0]}$, where $r_{[0]} = \frac{(g+g_1)\{1-(S_1+M_1)\}+g_1(\gamma S_1 - M_1)-(gS_1+d+v+\mu)}{1+g_1 M_1}$.

For the stability analysis of steady state interior equilibrium point is $L_*(S_*, I_*, M_*)$, we linearize the system (2.5) around L_* and obtain the corresponding Jacobian matrix

$$J_* = \begin{bmatrix} a_{11} & a_{12} & a_{13} \\ a_{21} & 0 & 0 \\ a_{31} & a_{32} & a_{33} \end{bmatrix},$$

where

$$\begin{aligned}
a_{11} = \frac{\partial F_1}{\partial S}|_{(S_*,I_*,M_*)} &= -\{r + g(S_* + I_*)\} + \{1 - (S_* + I_* + M_*)\}g - \gamma g_1 M_* - d - \lambda I_*, \\
a_{12} = \frac{\partial F_1}{\partial I}|_{(S_*,I_*,M_*)} &= -\{r + g(S_* + I_*)\} + \{1 - (S_* + I_* + M_*)\}g - \gamma g_1 M_* - \lambda S_* + \omega, \\
a_{13} = \frac{\partial F_1}{\partial M}|_{(S_*,I_*,M_*)} &= -\{r + g(S_* + I_*)\} - \gamma g_1 (S_* + I_*), \\
a_{21} = \frac{\partial F_2}{\partial S}|_{(S_*,I_*,M_*)} &= \lambda I_*, \\
a_{31} = \frac{\partial F_3}{\partial S}|_{(S_*,I_*,M_*)} &= -(\mu + g_1 M_*) + \gamma g_1 M_*, \\
a_{32} = \frac{\partial F_3}{\partial S}|_{(S_*,I_*,M_*)} &= -(\mu + g_1 M_*) + \gamma g_1 M_*, \\
a_{33} = \frac{\partial F_3}{\partial I}|_{(S_*,I_*,M_*)} &= \{1 - (S_* + I_* + M_*)\}g_1 - (\mu + g_1 M_*) + \gamma g_1 (S_* + I_*) - v.
\end{aligned}$$

The characteristic equation for J_* is

$$\mu^3 - Trace(J_*)\mu^2 + \Delta\mu - \frac{\partial (F_1, F_2, F_3)}{\partial (S, I, M)}|_{(S_*,I_*,M_*)} = 0, \tag{4.3}$$

where

$$\begin{aligned} Trace(J^*) &= a_{11}+a_{33}, \\ \Delta &= a_{11}a_{33}-a_{12}a_{21}-a_{13}a_{31}, \\ \frac{\partial(F_1,F_2,F_3)}{\partial(S,I,M)}|_{(S_*,I_*,M_*)} &= a_{12}a_{21}a_{33}-a_{13}a_{32}a_{21}. \end{aligned}$$

According to the Routh-Hurwitz criteria, the interior equilibrium point L_* is stable if $Trace(J_*)<0$, $\frac{\partial(F_1,F_2,F_3)}{\partial(S,I,M)}|_{(S_*,I_*,M_*)}<0$ and $Trace(J_*)\Delta<\frac{\partial(F_1,F_2,F_3)}{\partial(S,I,M)}|_{(S_*,I_*,M_*)}$.
We summarize the dynamics of system (2.5) in form of the following theorem.

Theorem 4.1 *In the absence of time lag ($\tau=0$), the stability of the system (2.5) around two equilibrium points can be described as follows:*
(i) The disease-free equilibrium point $L_1(S_1,0,M_1)$ of the system (2.5) is locally asymptotically stable for $R_0<1$, $r>r_{[0]}$ and $\frac{\partial(F_1,F_3)}{\partial(S,M)}|_{(S_1,0,M_1)}>0$, otherwise it is unstable;
(ii) The interior equilibrium point $L_*(S_*,I_*,M_*)$ of the system (2.5) is locally asymptotically stable for $Trace(J_*)<0$, $\frac{\partial(F_1,F_2,F_3)}{\partial(S,I,M)}|_{(S_*,I_*,M_*)}<0$ and $Trace(J_*)\Delta<\frac{\partial(F_1,F_2,F_3)}{\partial(S,I,M)}|_{(S_*,I_*,M_*)}$.

5. Analysis of the Model with Time Lag

5.1. Local stability analysis

The characteristic equation of the delayed system (2.5) around any equilibrium point $\widehat{L}=(\widehat{S},\widehat{I},\widehat{M})$ is given by

$$det\begin{bmatrix} -\{r+g(\widehat{S}+\widehat{I})\}+\{1-(\widehat{S}+\widehat{I}+\widehat{M})\}g & -\{r+g(\widehat{S}+\widehat{I})\}+\{1-(\widehat{S}+\widehat{I}+\widehat{M})\}g & -\{r+g(\widehat{S}+\widehat{I})\} \\ -\gamma g_1\widehat{M}-d-\lambda\widehat{I}-\lambda\widehat{I}e^{-\rho\tau}-\rho & -\gamma g_1\widehat{M}+\omega-\lambda\widehat{S}e^{-\rho\tau} & -\gamma g_1(\widehat{S}+\widehat{I}) \\ \lambda\widehat{I}e^{-\rho\tau} & -(d+e+\omega)+\lambda\widehat{S}e^{-\rho\tau}-\rho & 0 \\ -(\mu+g_1\widehat{M})+\gamma g_1\widehat{M} & -(\mu+g_1\widehat{M})+\gamma g_1\widehat{M} & \{1-(\widehat{S}+\widehat{I}+\widehat{M})\}g_1 \\ & & -(\mu+g_1\widehat{M})+\gamma g_1(\widehat{S}+\widehat{I})-v \end{bmatrix}=0. \tag{5.1}$$

The characteristic equation at $L_*(S_*,I_*,M_*)$ reduces to the following transcendental equation

$$\rho^3+A_1\rho^2+A_2\rho+A_3+(B_1\rho^2+B_2\rho+B_3)e^{-\rho\tau}=0, \tag{5.2}$$

where

$$\begin{aligned} A_1 &= -(l_{11}+l_{22}+l_{33}), \quad A_2 = l_{11}(l_{22}+l_{33})+l_{22}l_{33}+l_{13}l_{31}, \quad A_3 = l_{13}l_{31}l_{22}-l_{11}l_{22}l_{33}, \\ B_1 &= l_{11}^{'}-l_{12}^{'}, \quad B_2 = l_{11}l_{12}^{'}-l_{11}^{'}(l_{12}+l_{22})+l_{33}l_{12}^{'}-l_{33}l_{11}^{'}, \quad B_3 = l_{22}l_{33}l_{11}^{'}-l_{11}l_{33}l_{12}^{'} \\ &+ l_{12}l_{33}l_{11}^{'}-l_{13}l_{32}l_{11}^{'}+l_{13}l_{31}l_{12}^{'}, \end{aligned}$$

with

$$\begin{aligned} l_{11} &= -\{r+g(S_*+I_*)\}+\{1-(S_*+I_*+M_*)\}g-\gamma g_1M_*-d, \\ l_{12} &= -\{r+g(S_*+I_*)\}+\{1-(S_*+I_*+M_*)\}g-\gamma g_1M_*+\omega, \\ l_{13} &= -\{r+g(S_*+I_*)\}-\gamma g_1(S_*+I_*), \\ l_{22} &= -(d+e+\omega), \quad l_{31} = -(\mu+g_1M_*)+\gamma g_1M_*, \quad l_{32} = -(\mu+g_1M_*)+\gamma g_1M_*, \\ l_{33} &= \{1-(S_*+I_*+M_*)\}g_1-(\mu+g_1M_*)+\gamma g_1(S_*+I_*)-v, \\ l_{11}^{'} &= \lambda I_*, \quad l_{12}^{'} = \lambda S_*. \end{aligned}$$

It is well known that the delay-induced system (2.5) will be asymptotically stable at the equilibrium point $\widehat{L}$ if all characteristic roots of equation (5.1) have negative real parts. The equation (5.1) has

infinitely many eigenvalues due to a transcendental form. Thus, the classical Routh-Hurwitz criterion cannot be utilized for determining the stability of the system. For examining the stability nature, we need to verify the sign of the real parts of the zeros of (5.1). We assume that the equilibrium point $\widehat{L}$ of system (2.5) is asymptotically stable in the absence of time lag ($\tau = 0$). Next, we identify the condition(s) for which $\widehat{L}$ becomes unstable. Due to Rouche's theorem [53] and continuous nature with respect to τ, the necessary and sufficient condition(s) for the transcendental equation (5.1) to have roots with positive real parts is that it has purely complex zeros. Thus, we explore complex solutions for the equation (5.1) to find conditions for the switching of stbility.

Let $\mu(\tau) = u(\tau) + iw(\tau)$ be the eigenvalue of (5.1), where $u(\tau)$ and $w(\tau)$ are real numbers. If the equilibrium point $\widetilde{L}$ of the non-delayed system is stable, we must have $u(0) < 0$. Due to continuity nature, for a sufficiently small positive value of τ with the property $u(\tau) < 0$, $\widehat{L}$ remains stable in nature. The stability switching occurs at some particular positive magnitude of τ say $\widehat{\tau}$ for which $u(\widehat{\tau}) = 0$, $w(\widehat{\tau}) \neq 0$, that is, $\mu = iw(\widehat{\tau})$ is a purely imaginary zero of (5.1). Thus, $\widehat{L}$ is unstable for $u(\widehat{\tau}) > 0$. On the other hand, the equilibrium point $\widehat{L}$ is always stable when $w(\widehat{\tau})$ does not exist. In this case, the equation (5.1) does not have purely imaginary zeros for all τ.

In the absence of time lag ($\tau = 0$), the interior equilibrium point $L_*(S_*, I_*, M_*)$ of the system (2.5) is locally asymptotically stable when $Trace(J_*) < 0$, $\frac{\partial(F_1,F_2,F_3)}{\partial(S,I,M)}|_{(S_*,I_*,M_*)} < 0$ and $Trace(J_*)\Delta < \frac{\partial(F_1,F_2,F_3)}{\partial(S,I,M)}|_{(S_*,I_*,M_*)}$ (Theorem 4.1(ii)).
Next, we assume that $\rho = \xi + i\delta$ is the eigenvalue of the characteristic equation (5.2). Inserting this value in (5.2) and then separating real and imaginary parts, we respectively get

$$\begin{aligned}&\xi^3 - 3\xi\delta^2 + A_1(\xi^2 - \delta^2) + A_2\xi + A_3 + [\{B_1(\xi^2 - \delta^2) + B_2\xi + B_3\}\cos\delta\tau \\ &+(2B_1\xi\delta + \delta B_2)\sin\delta\tau]\mathrm{e}^{-\xi\tau} = 0,\end{aligned} \tag{5.3}$$

and

$$\begin{aligned}&3\xi^2\delta - \delta^3 + 2A_1\xi\delta + A_2\delta + [(2B_1\xi\delta + B_2\delta)\cos\delta\tau - \{(\xi^2 - \delta^2)B_1 \\ &+\xi B_2 + B_3\}\sin\delta\tau]\mathrm{e}^{-\xi\tau} = 0.\end{aligned} \tag{5.4}$$

A necessary criteria for a stability switching of L_* is that the characteristic equation (5.2) must have purely complex roots. We put $\xi = 0$ in (5.3) and (5.4) to obtain

$$A_3 - A_1\delta^2 = (B_1\delta^2 - B_3)\cos\delta\tau - \delta B_2\sin\delta\tau, \tag{5.5}$$

$$A_2\delta - \delta^3 = -B_2\delta\cos\delta\tau - (B_1\delta^2 - B_3)\sin\delta\tau. \tag{5.6}$$

Eliminating τ by squaring and adding (5.5) and (5.6), we get the equation in terms of δ as

$$\delta^6 + (A_1^2 - 2A_2 - B_1^2)\delta^4 + (A_2^2 - 2A_1A_3 - B_2^2 + 2B_1B_3)\delta^2 + (A_3^2 - B_3^2) = 0. \tag{5.7}$$

Substituting $\delta^2 = \vartheta$ in Eq. (5.7) leads to a cubic equation of the form

$$k(\vartheta) = \vartheta^3 + \kappa_1\vartheta^2 + \kappa_2\vartheta + \kappa_3 = 0, \tag{5.8}$$

where $\kappa_1 = (A_1^2 - 2A_2 - B_1^2)$, $\kappa_2 = (A_2^2 - 2A_1A_3 - B_2^2 + 2B_1B_3)$, $\kappa_3 = (A_3^2 - B_3^2)$.
From (5.8), we have

$$\frac{dk(\vartheta)}{d\vartheta} = 3\vartheta^2 + 2\kappa_1\vartheta + \kappa_2. \tag{5.9}$$

Solving

$$\frac{dk(\vartheta)}{d\vartheta} = 3\vartheta^2 + 2\kappa_1\vartheta + \kappa_2 = 0, \tag{5.10}$$

we obtain

$$\vartheta_{1,2} = \tfrac{1}{3}[-\kappa_1 \pm \sqrt{\kappa_1^2 - 3\kappa_2}]. \tag{5.11}$$

The zeros $\vartheta_{1,2}$ of (5.11) are negative or have negative real part when $\kappa_1 > 0$ and $\kappa_2 > 0$. Thus, the Eq. (5.10) has no positive zeros. If $\kappa_3 \geq 0$, then $k(0) = \kappa_3 \geq 0$ and $\lim_{\vartheta\to\infty} k(\vartheta) \to \infty$, which implies that (5.8) has only negative root(s). Moreover, if $\kappa_1 > 0$, $\kappa_2 > 0$ and $\kappa_3 \geq 0$, then there does not exist any δ for which $i\delta$ is a characteristic value of (5.2). Hence, the real parts of all characteristic values of (5.2) are negative $\forall\ \tau \geq 0$. In addition, if (a) $\kappa_1 > 0$ and $\kappa_2 < 0$, or (b) $\kappa_1 < 0$ and $\kappa_2 > 0$, or (c) $\kappa_3 < 0$, or (d) $\kappa_3 \geq 0$ and $\kappa_2 < 0$ holds, then (5.8) has at least one positive root ϑ_0. Consequently, Eq. (5.7) has at least one positive root, denoted by δ_0.
Thus, the characteristic Eq. (5.2) has a pair of purely complex zeros $\pm i\delta_0$. From (5.5) and (5.6), it follows that τ_p^* is a function of δ_0 for $p = 0, 1, 2, ...$, given by

$$\tau_p^* = \tfrac{1}{\delta_0} \arccos\left[\tfrac{(-A_1B_1+B_2)\delta_0^4+(-A_2B_2+A_1B_3+A_3B_1)\delta_0^2-A_3B_3}{(B_2\delta_0)^2+(-B_3+B_1\delta_0^2)^2}\right] + \tfrac{2\pi p}{\delta_0}. \tag{5.12}$$

Now, the system becomes locally asymptotically stable around the interior equilibrium point L_* for $\tau = 0$, if the condition (ii) of Theorem 4.1 is satisfied. According to Butler's lemma [54], L_* remain stable for $\tau < \tau^*$ with $\tau^* = \min_{p\geq 0} \tau_p^*$.
Next, we verify the transversality condition

$$\frac{d}{d\tau}\left[Re\{\rho(\tau)\}\right]_{\tau=\tau^*} \neq 0.$$

Differentiating (5.3) and (5.4) with respect to τ and putting $\xi = 0$ in the resulting expressions, we obtain

$$\begin{aligned} S(\delta)\frac{d\zeta}{d\tau} + B(\delta)\frac{d\delta}{d\tau} &= A(\delta), \\ -B(\delta)\frac{d\zeta}{d\tau} + S(\delta)\frac{d\delta}{d\tau} &= M(\delta), \end{aligned} \tag{5.13}$$

where

$$\begin{aligned} S(\delta) &= -3\delta^2 + A_2 + B_2\cos\delta\tau + 2B_1\delta\sin\delta\tau + \tau\left\{(\delta^2B_1 - B_3)\cos\delta\tau - \delta B_2\sin\delta\tau\right\}, \\ B(\delta) &= -2\delta A_1 - 2B_1\delta\cos\delta\tau + B_2\sin\delta\tau + \tau\left\{(\delta^2B_1 - B_3)\sin\delta\tau + \delta B_2\cos\delta\tau\right\}, \\ A(\delta) &= -\delta^2B_2\cos\delta\tau - (\delta^2B_1 - B_3)\delta\sin\delta\tau, \\ M(\delta) &= \delta^2B_2\sin\delta\tau - (\delta^2B_1 - B_3)\delta\cos\delta\tau. \end{aligned} \tag{5.14}$$

Solving the above system of equations, we obtain

$$\frac{d}{d\tau}\Big[Re\{\mu(\tau)\}\Big]_{\tau=\tau^*,\delta=\delta_0} = \Big[\frac{S(\delta)A(\delta) - B(\delta)M(\delta)}{S^2(\delta) + B^2(\delta)}\Big]_{\tau=\tau^*,\delta=\delta_0},$$

which indicates that $\frac{d}{d\tau}\Big[Re\{\mu(\tau)\}\Big]_{\tau=\tau^*,\delta=\delta_0} \neq 0$ when $S(\delta_0)A(\delta_0) - B(\delta_0)M(\delta_0) \neq 0$. Therefore, the transversality condition is satisfied and hence, the Hopf-bifurcation occurs when τ crosses through the critical value $\tau = \tau^*$.
Based on the foregoing discussion, we summarize the dynamics of the delay system (2.5) in form of the following theorem.

Theorem 5.1 *(i) In the absence of time lag ($\tau = 0$), the interior equilibrium point $L_*(M_*, I_*, M_*)$ of the system (2.5) is locally asymptotically stable. Further, if $\kappa_1 > 0$, $\kappa_2 > 0$, $\kappa_3 \geq 0$, then the interior equilibrium point L_* of the delay system (2.5) is asymptotically stable for all $\tau \in [0\ \infty)$.*
(ii) In the absence of time lag ($\tau = 0$), the interior equilibrium point $L_*(M_*, I_*, M_*)$ of the system (2.5) is locally asymptotically stable.
(iii) If $\kappa_1 > 0$ and $\kappa_2 < 0$, or $\kappa_1 < 0$ and $\kappa_2 > 0$, or $\kappa_3 < 0$, or $\kappa_3 \geq 0$ and $\kappa_2 < 0$ and $\vartheta_0 = \delta_0^2$ is a positive root of (5.8), then there exists $\tau = \tau^*$ for which the interior equilibrium point L_* of the delay system (2.5)

is asymptotically stable in $(0,\ \tau^*]$ *and unstable in* $(\tau^*,\ +\infty)$, *provided that* $S(\delta_0)A(\delta_0) - B(\delta_0)M(\delta_0) \neq 0$. *In addition, the system undergoes a Hopf-bifurcation at* L_* *when* τ *cross the threshold value* τ^*, *where*

$$\tau^* = \frac{1}{\delta_0}\arccos\left[\frac{(-A_1B_1 + B_2)\delta_0^4 + (-A_2B_2 + A_1B_3 + A_3B_1)\delta_0^2 - A_3B_3}{(B_2\delta_0)^2 + (B_3 - B_1\delta_0^2)^2}\right].$$

5.2. The direction and stability of Hopf bifurcating periodic solutions

In the last section, we obtained the sufficient conditions for the system (2.5) to experience Hopf-bifurcation at the interior equilibrium L_* when τ passes through the critical value τ^*. Here, we investigate the direction, stability and period of Hopf bifurcating periodic solutions at $\tau = \tau^*$ of the system (2.5) by applying the method of 'normal form theory' and 'center manifold theorem' due to Hassard et. al. [43].

We consider the following coordinate transformations:

$$z_1(t) = S(\tau t) - S_*,\ z_2(t) = I(\tau t) - I_*,\ z_3(t) = M(\tau t) - M_*,$$

where $\tau = \tau_0^* + \mu$ and μ is a real number. Then, the system (2.5) becomes a functional differential equation in $C = \mathbf{C}([-1, 0], \mathbf{R_+^3})$ given by

$$\dot{z}(t) = L_\mu(z_t) + F(\mu, z_t), \tag{5.15}$$

where $z(t) = (z_1(t), z_2(t), z_3(t))^T \in \mathbf{R^3}$. For any $\psi = (\psi_1, \psi_2, \psi_3)^T$ in $\mathbf{C}([-1, 0], \mathbf{R_+^3})$; the functions $L_\mu : \mathbf{C} \to \mathbf{R}$ and $F : \mathbf{R} \times \mathbf{C} \to \mathbf{R}$ are given by

$$L_\mu(\psi) = (\tau_0^* + \mu)A(\psi_1(0)\ \psi_2(0)\ \psi_3(0))^T + (\tau_0^* + \mu)B(\psi_1(-1)\ \psi_2(-1)\ \psi_3(-1))^T \tag{5.16}$$

and

$$F(\mu, \psi) = (\tau_0^* + \mu)C, \tag{5.17}$$

where $A = \begin{pmatrix} l_{11} & l_{12} & l_{13} \\ 0 & l_{22} & 0 \\ l_{31} & l_{32} & l_{33} \end{pmatrix}$, $B = \begin{pmatrix} -l_{11}^{'} & -l_{12}^{'} & 0 \\ l_{11}^{'} & l_{12}^{'} & 0 \\ 0 & 0 & 0 \end{pmatrix}$,

$$C = \begin{pmatrix} m_{11}\psi_1^2(0) + m_{12}\psi_2^2(0) + m_{13}\psi_1(0)\psi_2(0) + m_{14}\psi_1(0)\psi_3(0) + m_{15}\psi_2(0)\psi_3(0) \\ +m_{16}\psi_1(-1)\psi_2(-1) \\ \\ m_{21}\psi_1(-1)\psi_2(-1) \\ \\ m_{31}\psi_3^2(0) + m_{32}\psi_1(0)\psi_3(0) + m_{33}\psi_2(0)\psi_3(0) \end{pmatrix},$$

$$\begin{aligned} m_{11} &= m_{12} = -g, \quad m_{13} = -2g, \quad m_{14} = m_{15} = -(g + \gamma g_1), \quad m_{16} = -\lambda, \quad m_{21} = \lambda, \\ m_{31} &= -g_1, \quad m_{32} = m_{33} = (-g + \gamma g_1). \end{aligned}$$

Here, the system (2.5) experiences Hopf-bifurcation near L_* for $\mu = 0$. Applying the normal form theory and central manifold theorem as proposed by Hassard et al. [43], we have the following theorem.

Theorem 5.2 *Suppose that the condition (ii) of Theorem 5.1 is satisfied for the system (2.5). If* $\mu_2 < 0$ $(\mu_2 > 0)$, *then the Hopf bifurcating periodic solution is subcritical (supercritical) for* $\tau < \tau_0^*$ $(\tau > \tau_0^*)$. *If* $\beta_2 > 0$ $(\beta_2 < 0)$, *then the bifurcating periodic solution is orbitally unstable (stable). Moreover,* τ_2 *represents the period of the bifurcating periodic solution and the period decreases (increases) for* $\tau_2 < 0$ $(\tau_2 > 0)$.

Proof: See the Appendix A. □

Table 1: The set of values of parameters for numerical simulation

Parameter	Ecological meaning	Values	Sources
r	recruitment rate of coral	0.07	Briggs *et al.* (2018) [42]
g	combined rate of local recruitment including the lateral growth of coral over free space	0.1	Briggs *et al.* (2018) [42]
g_1	combined rate of local recruitment and lateral growth of macroalgae over free space	0.4	Briggs *et al.* (2018) [42]
d	death rate of coral	0.05	Briggs *et al.* (2018) [42]
μ	recruitment rate of macroalgae	0.1	–
v	death rate of macroalgae	0.5	Briggs *et al.* (2018) [42]
λ	disease transmission rate	0.1	–
ω	rate of infected coral colonies revert to the susceptible class due to regeneration of tissue	0.01	–
e	additional mortality rate of infected coral due to infection	0.01	–
γ	dimensionless parameter $(0 < \gamma \leq 1]$	0.6	Briggs *et al.* (2018) [42]

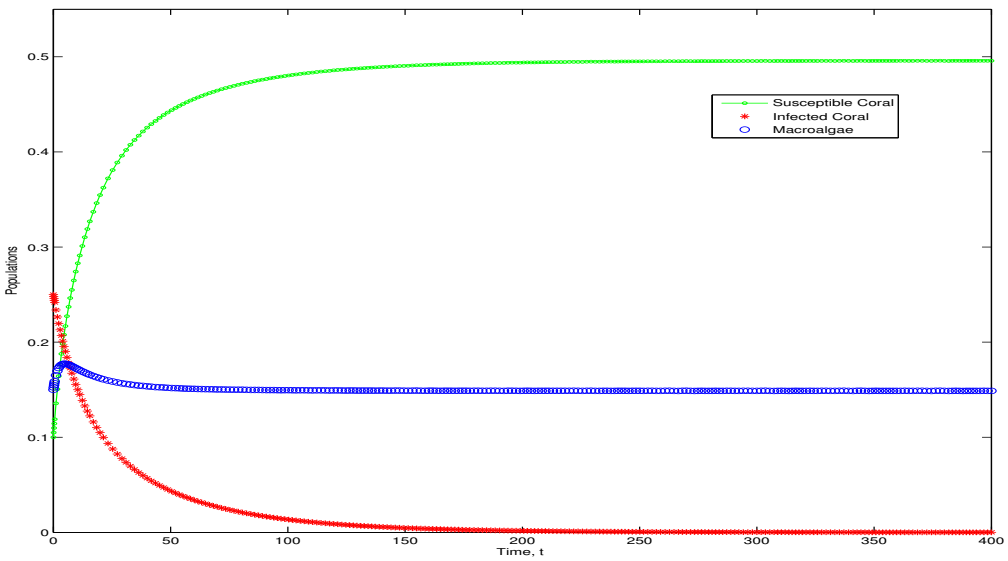

Figure 1: Numerical simulation in the absence of delay for system (2.5). The parameter values are $r = 0.07$; $g = 0.1$; $g_1 = 0.4$; $d = 0.05$; $\mu = 0.1$; $v = 0.5$; $\lambda = 0.1$; $\omega = 0.01$; $e = 0.01$; $\gamma = 0.6$; $\tau = 0$; [.10 .250 .15] (see Table 1).

6. Numerical Investigations

In this section, we perform some numerical experiments on the system (2.5) to check the feasibility of our analytical findings concerning the stability criteria. We focus on the role of vital parameters: disease transmission rate λ, conversion rate ω of infected colonies to healthy class and time lag τ due to incubation in the coral-reef system. In our numerical computation, we utilize MATLAB and MATHEMATICA and choose the biologically feasible parameter values from the previous published works as indicated in the Table 1, that is, $r = 0.07$; $g = 0.1$; $g_1 = 0.4$; $d = 0.05$; $\mu = 0.1$; $v = 0.5$; $\lambda = 0.1$; $\omega = 0.01$; $e = 0.01$; $\gamma = 0.6$; and the initial species sizes are $[S(0), I(0), M(0)] = [0.10,\ 0.25,\ 0.15]$. In the absence of time lag, we have verified that the criteria for the existence and stability of disease free equilibrium L_1 of system (2.5) is satisfied. For $\lambda = 0.1$ and the values of rest of the parameters from Table 1, we have disease

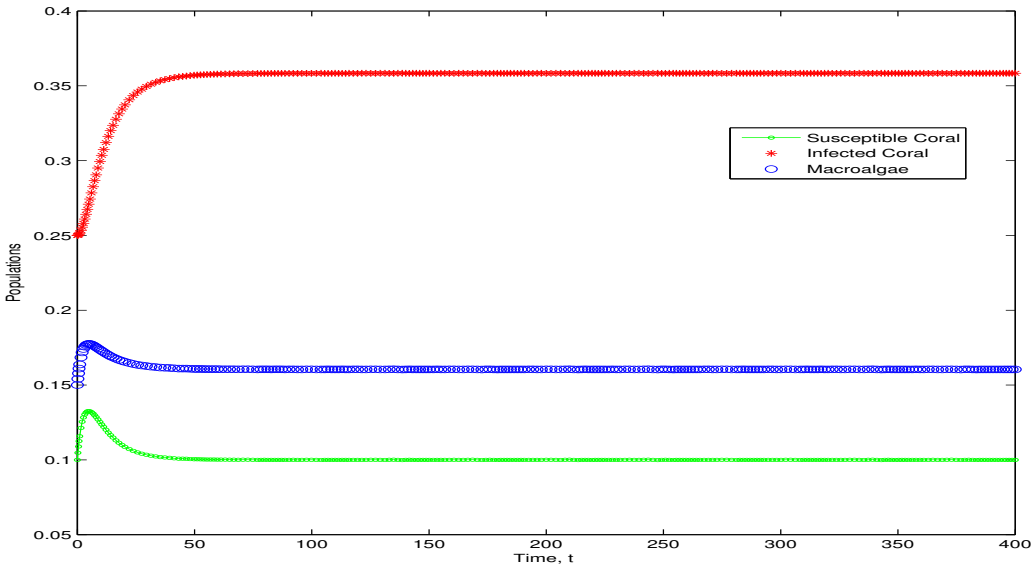

Figure 2: Numerical simulation for $\lambda = 0.7$ in the absence of delay for system (2.5). The rest parameter values are taken as in the Figure 5.2

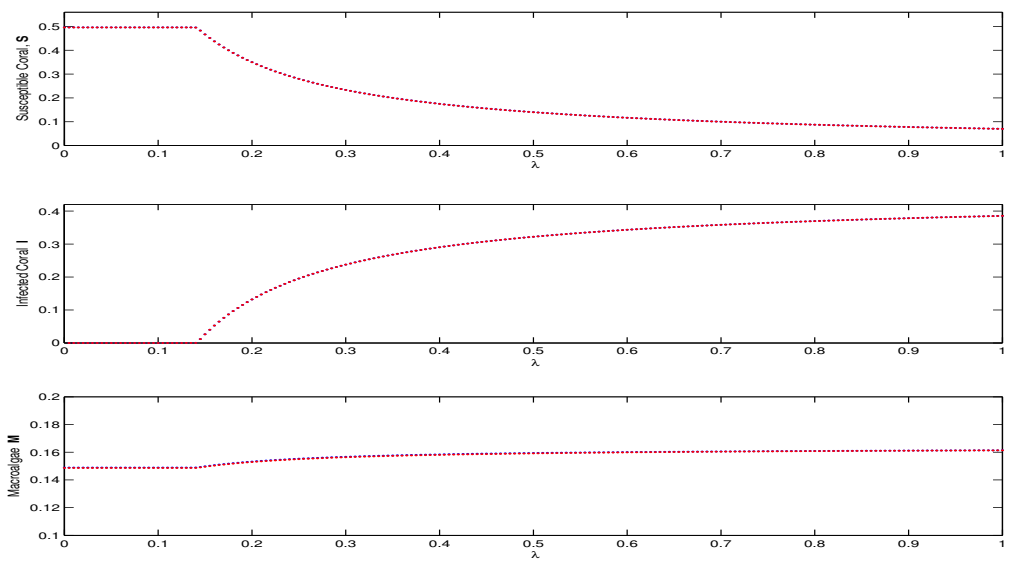

Figure 3: Bifurcation diagram of system (2.5) for λ. The parameter values are taken as in the Figure 5.2.

free equilibrium point $L_1(0.495832, 0, 0.148789)$ and $g_1^0 = gM_1 + v + \mu(1 - \frac{1}{M_1}) = -0.0572138$. Thus, the admissible criterion: $g_1(0.4) > g_1^0(-0.0572138)$ for disease free equilibrium point L_1 is satisfied. Using the same set of the values of parameters, we have computed the disease threshold parameter $R_0 = 0.708331 < 1$ ($R_0 = \frac{\lambda S_1}{d+e+\omega}$), $r > r_{[0]} = -0.436435$ and $\frac{\partial(F_1,F_3)}{\partial(S,M)}|_{(S_1,0,M_1)} = 0.038086 > 0$. Moreover, eigenvalues associated with $L_1(0.495832, 0, 0.148789)$ are -0.490466, -0.077653, -0.0204168.

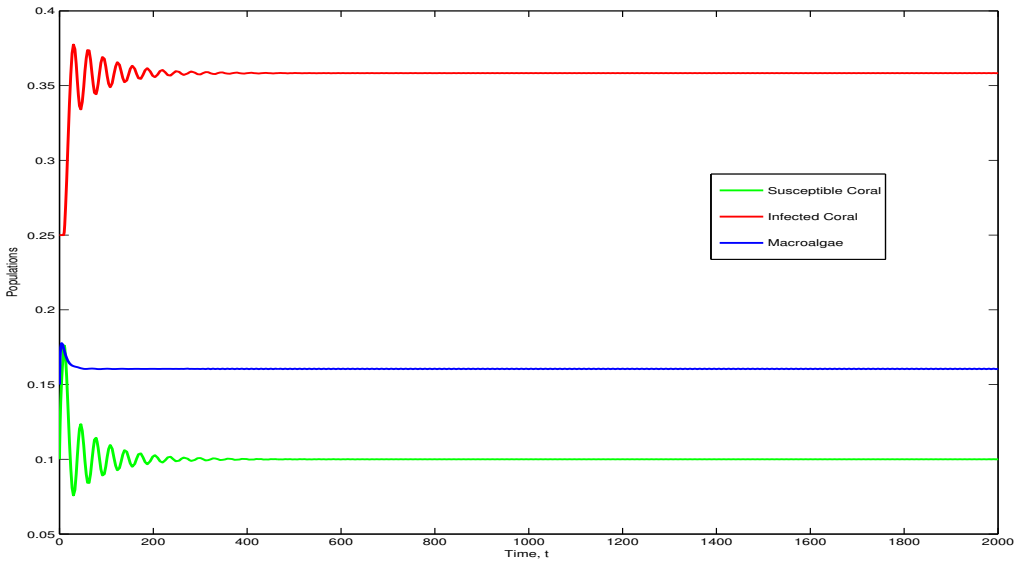

Figure 4: Numerical simulation in the presence of delay $\tau = 9.0$ for system (2.5). The parameter values are taken as in the Figure 2.

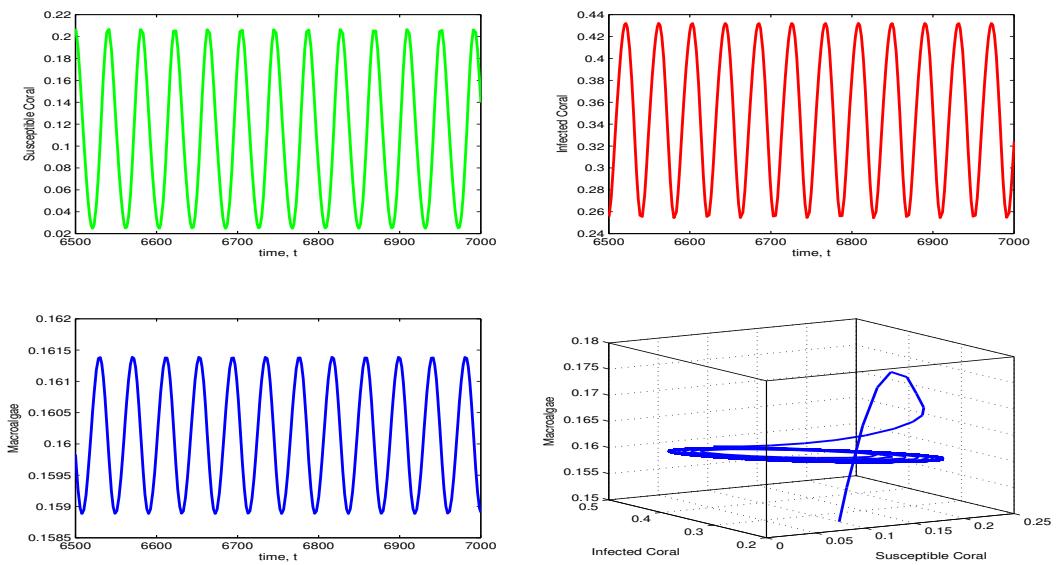

Figure 5: Numerical simulation for $\tau = 12.548$ in the presence of delay for system (2.5). The other parameter values as in Figure 2.

Due to Theorem 4.1, in the absence of time lag (τ), the system is locally asymptotically stable around L_1. In this case, disease does not spread among the coral reef system as the healthy coral and macroalgae species coexist in the locally asymptotically stable position around the disease free equilibrium point (see Figure 5.2). Further, the disease persists among the coral-reef populations when the rate of disease

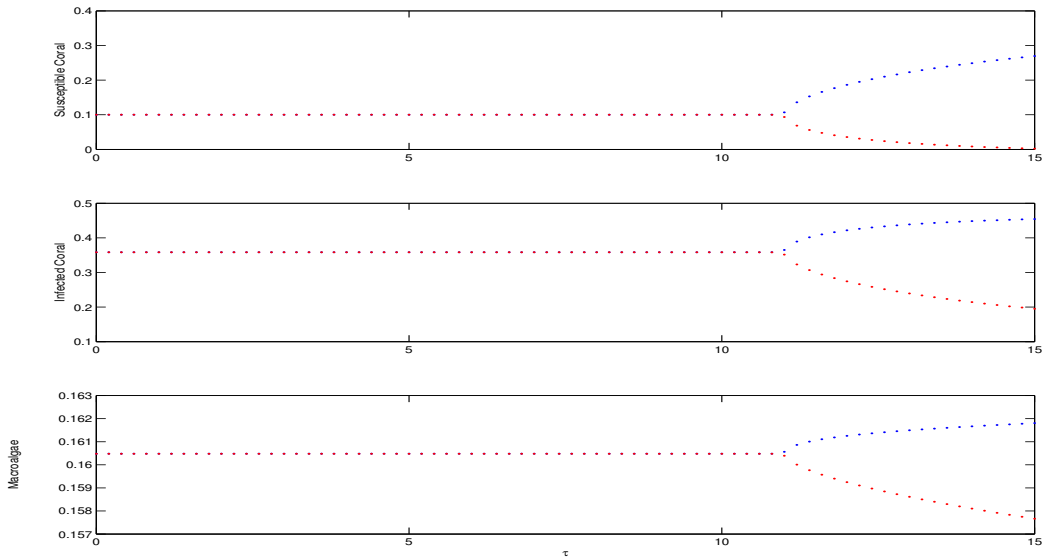

Figure 6: Bifurcation diagram of system (2.5) for time delay τ. The parameter values are taken as in the Figure 2.

transmission λ transcends to a critical magnitude. From Figure 2, one can observe that all the species coexist in a stable position around the interior equilibrium point L_* for $\lambda = 0.7$. In this case, the disease threshold parameter $R_0 = 4.95832 > 1$, so the disease spreads among the coral reef populations. In the absence of time lag, our numerical simulation shows that a minimum force of infection ($\lambda_{min} \approx 0.1412$) is required to disseminate the disease in the coral reef species of the system (2.5). For a more clear dynamics of the system, we draw the diagram (Figure 3) for different values of λ. It is also imperative to mention that a transcritical bifurcation happens for gradually enhancing the magnitude of λ through λ_{min}, that is, the disease-free equilibrium loses stability, and the interior equilibrium point becomes stable in nature at λ_{min}. Similar observations have been reported by the authors in [35,36,37,34].

Next, we study the impact of time lag on the disease dynamics. To attain our goal, we fix $\lambda = 0.7$ with the other values of parameters given in the Table 1. The interior equilibrium point takes the form $L_*(S_*, I_*, M_*)$ with species densities $S_* = 0.1, I_* = 0.358343, M_* = 0.160479$. It is observed that the interior equilibrium point L_* is stable in nature in the absence of time lag ($\tau = 0$). If we introduce the time lag in the system, we notice that for $\tau = 9.0$, all the species coexist in the locally asymptotically stable position around the interior equilibrium point (see Fig.4), since $Trac(J_*) = -0.81879 < 0$, $\frac{\partial(F_1,F_2,F_3)}{\partial(S,I,M)}|_{(S_*,I_*,M_*)} = -0.0106389 < 0$ and $Trace(J_*)\Delta[-0.150141] < \frac{\partial(F_1,F_2,F_3)}{\partial(S,I,M)}|_{(S_*,I_*,M_*)}[-0.0106389]$. With the same set of parameters values, we get $\kappa_1 = 0.104442$, $\kappa_2 = 0.00657864$, $\kappa_3 = -0.0000559973$, which reveals the existence of a positive zero, $\vartheta_0 \approx 0.00754336$ of the Eq. (5.8). As a result, (5.7) has at least one positive zero, namely, $\delta_0 \approx 0.0868525$. Due to Theorem 5.1, we notice that the stability switching may arise as τ increases. The value of τ for which stability switching occurs is $\tau^* \approx 10.919$ and it can easily be calculated from (5.5) and (5.6). In addition, we have checked numerically that $S(\delta_0)A(\delta_0) - B(\delta_0)M(\delta_0) = 0.000156696 \neq 0$, which ensures the transversality condition: $\frac{d}{d\tau}\left[Re\{\rho(\tau)\}\right]_{\tau=\tau^*} = 0.00562687 \neq 0$. According to Butler's lemma, L_* remains stable for $\tau < \tau^*$ as Figure 4 depicts which corresponds to a solution of the system (5.5) for $\tau = 9.0$. If the magnitude of τ enhances through $\tau^*(\approx 10.919)$, a periodic solution arises which is the case of Hopf-bifurcation (Figure 5). It is also revealed that the amplitude of oscillations of the system increases with increase in τ when the magnitude of τ is greater than τ^*. This observation is in agreement with the result of Bhattacharyya et

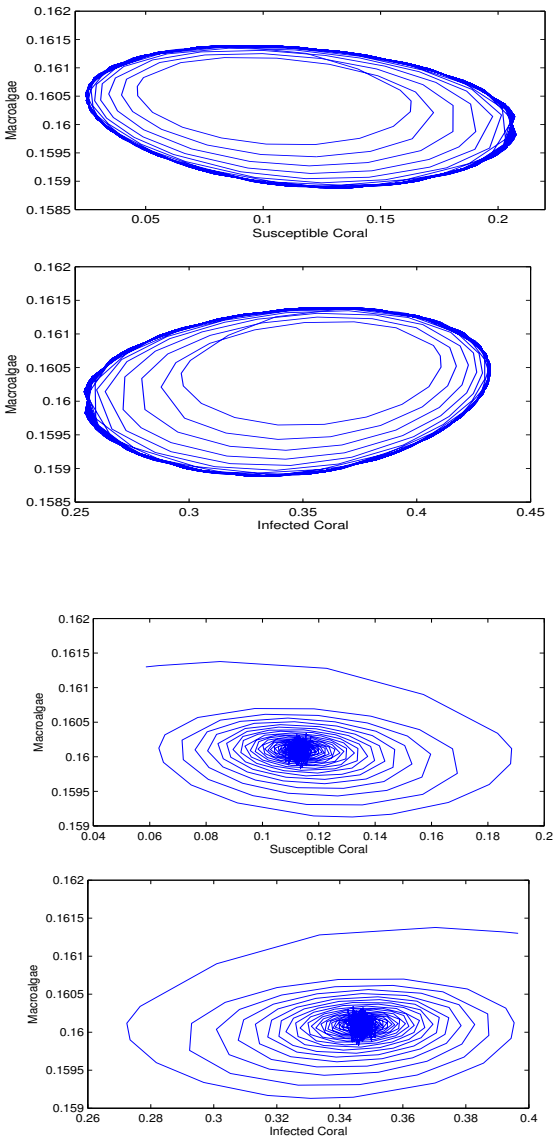

Figure 7: Numerical simulation of system (2.5) for $\omega = 0.01$ in of delay of the system (2.5). (b) Numerical simulation of system (2.5) for $\omega = 0.019$. The other parameters values are same as in Figure 5.

. al. [38]. For a clear dynamics of the coral reef system, we draw a bifurcation diagram (Figure 6) by varying the values of time delay τ.

Further, utilizing the algorithms described in Section 5.3, we obtain $C_1(0) = -0.006698 - 0.08857i$ for $\tau = \tau^*$, which yields $\mu_2 = 1.190359$, $\beta_2 = -0.013396$ and $\tau_2 = 0.086$. So, the Hopf-bifurcation of the system (2.5) around the interior equilibrium point $L_*(0.1, 0.358343, 0.160479)$ is supercritical. The bifurcating periodic solution appears for $\tau > \tau^*$, and it is orbitally stable, and the period of periodic solution accelerate with an increase in τ. The importance of Hopf-bifurcation in this context is that a limit cycle is formed around the fixed point L_* at the bifurcation point. In this case, two distinct solutions originating from two different initial values converge to the limit cycle, which results into a stable periodic solution.

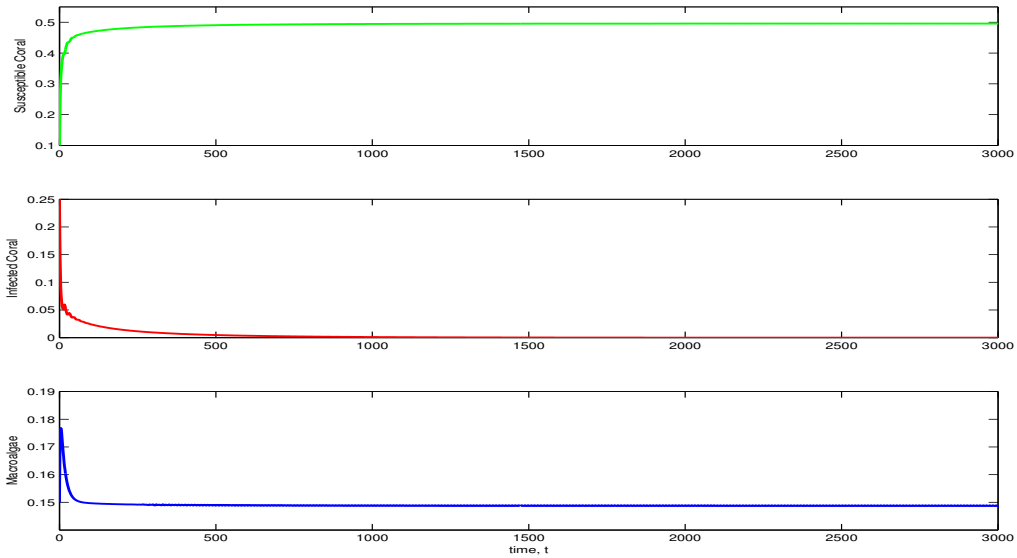

Figure 8: Population abundances for $\omega = 0.30$ in of delay of the system (2.5) and other parameter values are same as in Figure 5.

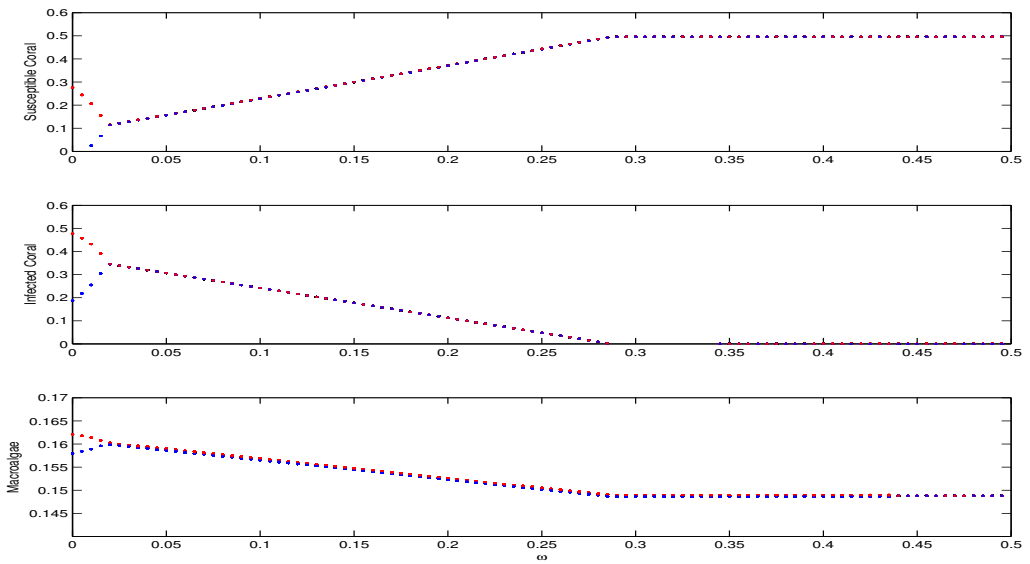

Figure 9: Bifurcation diagram of system (2.5) for time delay ω. The parameter values are taken as in the Figure 5.

We also describe the effect of conversion rate ω of infected colonies to healthy class on the disease dynamics of the system (2.5). To demonstrate the impact of ω in the system, we slowly increasing the the magnitude of ω and settle the value of τ at 12.648 and remaining parameter values are same as in the Figure 2. For $\omega = 0.019$, the interior equilibrium point is stable focus. For sufficiently higher value

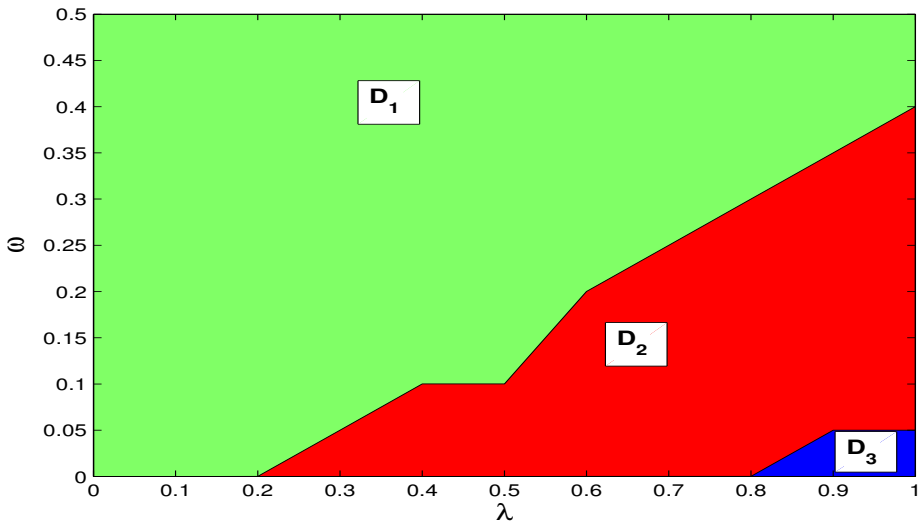

Figure 10: Domains of stability and instability of the model (2.5) in two dimensional $\lambda - \omega$ parameter space where other parameter values are fixed as in Table 1. The horizontal axis represents the rate of disease transmission λ and the vertical axis represent recovery rate ω. The D_1 (green) domain depicts that the disease-free equilibrium point $L_1(S_1, 0, M_1)$ is stable; the D_2 (red) domain indicates the stability region of the interior equilibrium point $L_*(S_*, I_*, M_*)$ and the D_3 (blue) domain depicts oscillatory nature around interior equilibrium L_*.(Color figure online)

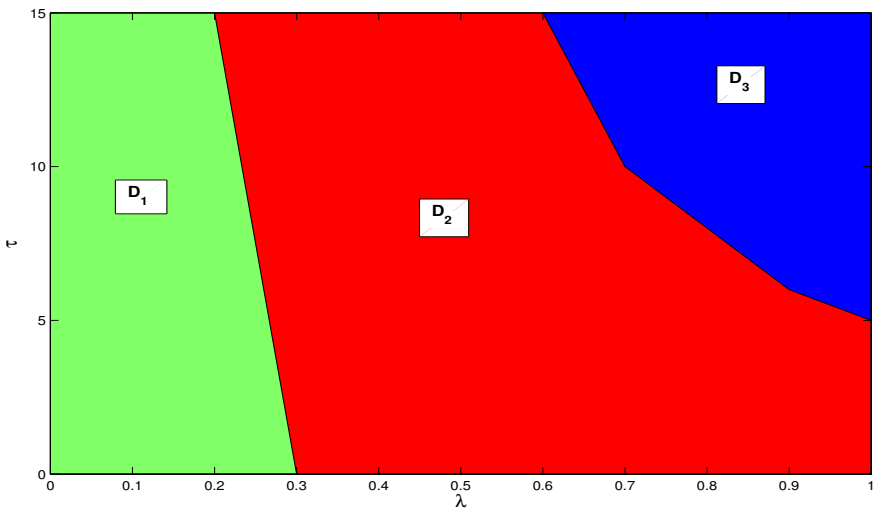

Figure 11: Domains of stability and instability of the model (2.5) in two dimensional $\lambda - \tau$ parameter space where other parameter values are fixed as in Table 1. The horizontal axis represents the rate of disease transmission λ and the vertical axis represent recovery rate ω. The D_1 (green) domain depicts that the disease-free equilibrium point $L_1(S_1, 0, M_1)$ is stable; the D_2 (red) domain indicates the stability region of the interior equilibrium point $L_*(S_*, I_*, M_*)$ and the D_3 (blue) domain depicts oscillatory nature around interior equilibrium L_*.(Color figure online)

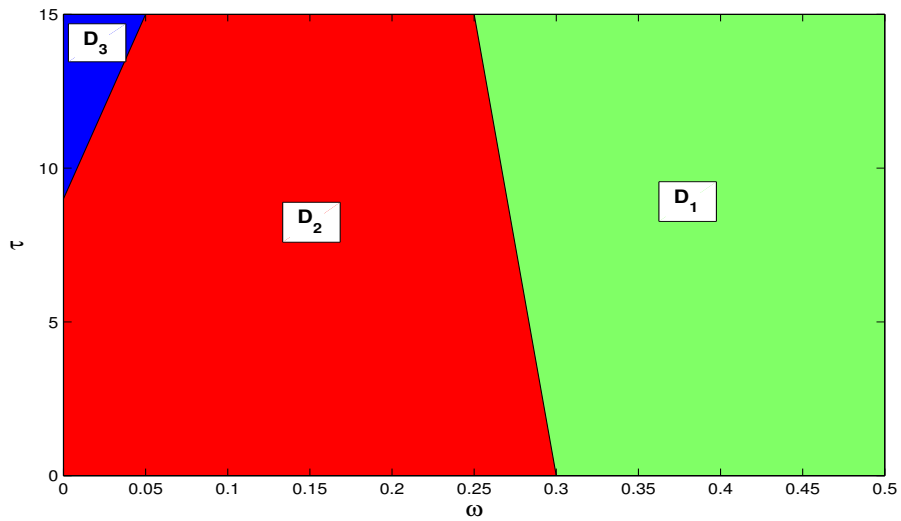

Figure 12: Domains of stability and instability of the model (2.5) in two dimensional $\omega - \tau$ parameter space where other parameter values are fixed as in Table 1. The horizontal axis represents the rate of disease transmission λ and the vertical axis represent recovery rate ω. The D_1 (green) domain depicts that the disease-free equilibrium point $L_1(S_1, 0, M_1)$ is stable; the D_2 (red) domain indicates the stability region of the interior equilibrium point $L_*(S_*, I_*, M_*)$ and the D_3 (blue) domain depicts oscillatory nature around interior equilibrium L_*.(Color figure online)

of $\omega > \omega_0[\approx 0.0181]$, can control the oscillation among the species due to presence of time lag. If we further steadily enhance the magnitude of ω, it is observe that ω control the spread of disease among the coral reef ecosystem for sufficiently more higher value of $\omega > \omega_c[\approx 0.288]$. Thus a transcritical bifurcation occur between interior and disease-free equilibrium point at ω_c. So, effect of conversion rate ω of infected colonies to healthy class can control the oscillation among the system, and control disease transmission among coral species.

For a clear understanding of the stability dynamics of the model (2.5), we produce two parameter bifurcation diagrams (Fig. [10-12]) in terms of the stability and instability domain around the equilibrium points L_1 and L_*. In Fig. [10-12], the green domain (D_1) delineates the stability region of disease-free equilibrium point L_1, the red domain (D_2) represents the stability region of the interior equilibrium point L_*, while the blue domain (D_3) indicates one periodic oscillation nature of the system around the equilibrium point L_*. Initially, we trace two parameter bifurcation in $\lambda - \omega$ space (see the Fig 10). We observe that for arbitrary value of ω, the system exhibits stable behavior around the disease-free equilibrium point L_1 when the rate of disease transmission (λ) is less than a critical value (≈ 0.2). For sufficiently moderate to higher value of ω and for the disease transmission rate (λ) crossing a critical value (≈ 0.2), the system shows stable nature around L_*. Consequently, the disease persists among the species of coral reef system. On the other hand, all species of the system indicate oscillation nature around L_* for a sufficiently higher value of λ and a sufficiently smaller value of ω. Subsequently, we produce the stability and oscillation domain of the model (2.5) in $\lambda - \tau$ parameter space (see the Fig. 11). From Fig. 11, we observe that for any moderate value λ up to (≈ 0.3) and arbitrary value of time lag τ, the model (2.5) exhibits stable nature around the equilibrium L_* and the coral species become disease-free. It is also observe that the disease persists among the coral species with stable nature for sufficiently moderate to higher value of λ and arbitrary value of time lag τ. On the other hand, the species show the periodic nature around the interior equilibrium point L_* when disease transmission rate λ is quite high and the magnitude of time lag τ between sufficiently moderate to high values. Further, we draw domain of the species dynamics for the system (2.5) in $\omega - \tau$ parameter space. From Fig. 12, one can observe the model indicates the oscillation nature among the all species when the recovery rate ω and the magnitude of time

lag τ are sufficiently low and high respectively. For any value of time lag τ and for sufficiently moderate value of ω, the periodic oscillation around the interior equilibrium L_* disappears and the system becomes unstable from its stable nature around L_*. Next, if the magnitude of ω is high enough, then the system switches form oscillation around interior equilibrium point L_* to stable nature around the disease free equilibrium point L_1 for an arbitrary magnitude of time lag τ. The above observations indicate that the time lag τ can produce the oscillation among the species whereas the conversion efficiency or recovery rate ω can control the oscillation among the system as well as disease transmission among coral species.

7. Conclusion

It is well known that time lag is an important factor in the investigation of biological processes as the behavior of the corresponding system does not exhibit it instantly. Thus, it is of significant interest to analyze the impact of time lag on the stability of the coral reef system. Coral disease is also one of the vital causes of coral degeneration, so it is necessary to incorporate it in the study of coral reef system. In the present article, we have proposed and analyzed a coral reef epidemiological system in terms of 3D coupled ordinary differential equations of susceptible-infective coral and macroalgae. In the presence of disease in coral, the coral population is subdivided into two distinct sets, namely healthy and infected. The healthy coral turns into infected through a contagious pathway (e.g, black band and white band diseases). The healthy coral does not become infected instantaneously but it is induced by time delay due to the incubation. Disease transmission process follows the principle of mass-action. Hence, it is imperative to consider the effects of disease transmission rate (λ), incubation time lag (τ), and conversion/recovery rate (ω) in the coral reef dynamical system.

We have analyzed the biologically feasible distinct equilibrium points of the system. The preliminary result, presented in Section 3, is concerned with the existence and positivity of solutions of (2.5). We computed the disease basic reproduction number R_0 and threshold parameter $r_{[0]}$ for recruitment rate of coral. Analytical results show that the disease-free equilibrium is locally asymptotically stable when $R_0 < 1$ and $r > r_{[0]}$ provided that $\frac{\partial(F_1,F_3)}{\partial(S,M)}|_{(S_1,0,M_1)}$ is positive definite. This result illustrates that the disease will spread among the corals when the rate of disease transmission (λ) is above some critical value because R_0 is a monotone increasing function of λ. On the contrary, a sufficiently higher recovery rate (ω) of coral reef is necessary to wipe out the disease from system as R_0 is monotone decreasing function with increasing value of recovery rate ω. Thus, the disease transmission rate spreads the disease in the system whereas the recovery rate plays a key role in controlling the spread of disease propagation in the coral reef ecosystem. In the presence of time delay (τ), it is observed that the system shows stable (unstable) nature when the delay is less (greater) than a threshold value (τ^*). Thus, the system experiences a Hopf-bifurcation around L_*. We have presented the criteria for existence of Hopf-bifurcation around L_*. Moreover, it is observed that the oscillation among the corals can be controlled when the conversion efficiency rate (ω) crosses a threshold value. Also, one can notice that the magnitude of ω increases when the system becomes disease free. Applying the notation of Hassard et al., we have explored the direction of Hopf-bifurcation, stability and period of the bifurcating periodic solution.

The results obtained in this study suggest that the conversion efficiency or recovery rate and incubation delay time play a crucial role in controlling the disease transmission and oscillations among the species of coral-reef ecosystem. The introduction of incubation delay in a coral reef ecosystem demonstrates that the all species coexist in oscillatory nature. In fact, the conversion or recovery rate of infected colonies to healthy coral can prevent the oscillation among the species of the system and control the disease transmission among coral species.

Acknowledgments

Buddhadev Ranjit is supported by research fellowship (SRF) from Council of Scientific and Industrial Research (CSIR), Govt. of India, File No. 09/096(0950)/2018-EMR-I.

Compliance with ethical standards

Conflicts of interest: the authors declare that there is no conflict of interests regarding the publication of this article.

Ethical standard: the authors state that this research complies with ethical standards. This research does not involve either human participants or animals.

Data availability statements: all data generated or analyzed during this study are included in this article.

References

1. Cole, A. J., Pratchett, M. S., & Jones, G. P. (2008). Diversity and functional importance of coral-feeding fishes on tropical coral reefs. *Fish and Fisheries*, **9**(3), 286-307.
2. Connell, J.H.: Diversity in tropical rain forests and coral reefs: high diversity of trees and corals is maintained only in a nonequilibrium state. Science 199(4335), 1302-1310 (1978)
3. Smith, S.V., Buddemeier, R.: Global change and coral reef ecosystems. Annual Review of Ecology and Systematics 23(1), 89-118 (1992)
4. Peterson, C., Lubchenco, J.: On the value of marine ecosystems to society. Nature's Services. Societal Dependence on Natural Ecosystems. Island Press, New York, 177-194 (1997)
5. Spalding, M., Grenfell, A.: New estimates of global and regional coral reef areas. Coral reefs 16(4), 225-230 (1997)
6. Mcallister, D.E.: What is the status of the worlds coral reef fishes. Sea Wind 5(1), 14-18 (1991)
7. Salvat, B.: Coral reefs a challenging ecosystem for human societies. Global environmental change 2(1), 12-18 (1992)
8. Richmond, R.H.: Coral reefs: present problems and future concerns resulting from anthropogenic disturbance. American Zoologist 33(6), 524-536 (1993)
9. Wilkinson, C.R.: Global change and coral reefs: impacts on reefs, economies and human cultures. Global Change Biology 2(6), 547-558 (1996)
10. Weil, E.: Coral reef diseases in the wider caribbean. In: Coral Health and Disease, 35-68. Springer, (2004)
11. Peters, E.C.: Diseases of coral reef organisms. In: Coral Reefs in the Anthro-pocene, 147-178. Springer, (2015)
12. Wilkinson, C.R., Buddemeier, R.W.: Global Climate Change and Coral Reefs: Implications for People and Reefs: Report of the UNEP-IOC-ASPEI-IUCN Global Task Team on the Implications of Climate Change on Coral Reefs. IUCN, (1994)
13. Roberts, C.M.: Effects of fishing on the ecosystem structure of coral reefs. Conservation biology 9(5), 988-995 (1995)
14. Shore, A., Caldwell, J.M.: Modes of coral disease transmission: how do diseases spread between individuals and among populations Marine Biology 166(4), 1-14(2019)
15. Bruckner, A.W., Bruckner, R.J., Williams Jr, E.H.: Spread of a black-band disease epizootic through the coral reef system in st. anns bay, jamaica. Bulletin of Marine Science 61(3), 919-928 (1997)
16. Zettler, E.R., Mincer, T.J., Amaral-Zettler, L.A.: Life in the plastisphere: microbial communities on plastic marine debris. Environmental science & technology 47(13), 7137-7146 (2013)
17. Goldstein, M.C., Carson, H.S., Eriksen, M.: Relationship of diversity and habitat area in north pacific plastic-associated rafting communities. Marine Biology 161(6), 1441-1453 (2014)
18. Lamb, J.B., Willis, B.L., Fiorenza, E.A., Couch, C.S., Howard, R., Rader, D.N., True, J.D., Kelly, L.A., Ahmad, A., Jompa, J., et al.: Plastic waste associated with disease on coral reefs. Science 359(6374), 460-462 (2018)
19. Page, C., Willis, B.: Epidemiology of skeletal eroding band on the great barrier reef and the role of injury in the initiation of this widespread coral disease. Coral Reefs 27(2), 257-272 (2008)
20. Gignoux-Wolfsohn, S., Marks, C.J., Vollmer, S.V.: White band disease transmission in the threatened coral, acropora cervicornis. Scientific reports 2(1), 1-3(2012)
21. Wolf, A.T., Nugues, M.M.: Synergistic effects of algal overgrowth and corallivory on caribbean reef-building corals. Ecology 94(8), 1667-1674 (2013)
22. Katz, S.M., Pollock, F.J., Bourne, D.G., Willis, B.L.: Crown-of-thorns starfish predation and physical injuries promote brown band disease on corals. CoralReefs 33(3),705-716 (2014)
23. Rotjan, R.D., Lewis, S.M.: Impact of coral predators on tropical reefs. Marine ecology progress series 367, 73-91 (2008)
24. Nicolet, K., Hoogenboom, M.O., Gardiner, N., Pratchett, M., Willis, B.: The corallivorous invertebrate drupella aids in transmission of brown band disease on the great barrier reef. Coral Reefs 32(2), 585-595 (2013)
25. Sussman, M., Loya, Y., Fine, M., Rosenberg, E.: The marine fireworm hermodice carunculata is a winter reservoir and spring-summer vector for the coral-bleaching pathogen vibrio shiloi. Environmental Microbiology 5(4), 250-255 (2003)

26. Grober-Dunsmore, R., Bonito, V., Frazer, T.K.: Potential inhibitors to recovery of acropora palmata populations in st. john, us virgin islands. Marine Ecology Progress Series 321, 123-132 (2006)

27. Greene, A., Donahue, M.J., Caldwell, J.M., Heron, S.F., Geiger, E., Raymundo, L.J.: Coral disease time series highlight size-dependent risk and other drivers of white syndrome in a multi-species model. Frontiers in Marine Science 7, 601469 (2020)

28. Bruno, J.F., Selig, E.R., Casey, K.S., Page, C.A., Willis, B.L., Harvell, C.D., Sweatman, H., Melendy, A.M.: Thermal stress and coral cover as drivers of coraldisease outbreaks. PLoS biology 5(6), 124 (2007)

29. Rosenberg, E., Falkovitz, L.: The vibrio shiloioculina patagonica model system of coral bleaching. Annual review of microbiology 58, 143 (2004)

30. McClanahan, T.R., McLaughlin, S.M., Davy, J.E., Wilson, W.H., Peters, E.C., Price, K.L., Maina, J.: Observations of a new source of coral mortality along the kenyan coast. Hydrobiologia 530(1), 469-479 (2004)

31. Kuta, K., Richardson, L.: Ecological aspects of black band disease of corals: relationships between disease incidence and environmental factors. Coral Reefs 21, 393-398 (2002)

32. Jones, R.J., Bowyer, J., Hoegh-Guldberg, O., Blackall, L.L.: Dynamics of a temperature-related coral disease outbreak. Marine Ecology Progress Series 281,63-77 (2004)

33. Zvuloni, A., Artzy-Randrup, Y., Stone, L., Kramarsky-Winter, E., Barkan, R., Loya, Y.: Spatio-temporal transmission patterns of black-band disease in a coral community.PLoS One 4(4), 4993 (2009)

34. Biswas S, Ahmad B, Khajanchi S. Exploring dynamical complexity of a cannibalistic eco-epidemiological model with multiple time delay. Mathematical Methods in the Applied Sciences, 46(4), 4184-4211 (2023)

35. Bhattacharyya J, Pal S. Stage-structured cannibalism with delay in maturation and harvesting of an adult predator. Journal of Biological Physics, 39, 37-65 (2013)

36. Biswas S, Samanta S, Chattopadhyay J. Cannibalistic predator-prey model with disease in predator - a delay model. International Journal of Bifurcation and Chaos, 25(10), 1550130 (2015)

37. Biswas S, Samanta S, Khan QJA, Chattopadhyay J. Effect of multiple delays on the dynamics of cannibalistic prey-predator system with disease in both populations. International Journal of Biomathematics, 10(04), 1750049 (2017)

38. Bhattacharyya, J., Pal, S.: Microbial disease in coral reefs: an ecosystem in transition. Discrete & Continuous Dynamical Systems-B 21(2), 373 (2016)

39. M. Sardar, S. Biswas, S. Khajanchi, The impact of distributed time delay in tumor-immune interaction system. Chaos, Solitons and Fractals, 142, 110483 (2021)

40. Exploring the dynamics of a tumor-immune interplay with time delay Sardar M., Khajanchi S., Biswas S., Abdelwahab S.F., Nisar K.S. Alexandria Engineering Journal, 60(5), 4875-4888 (2021)

41. Blackwood, J.C., Hastings, A.: The effect of time delays on caribbean coral'algal interactions. Journal of Theoretical Biology 273(1), 37-43 (2011)

42. Briggs CJ, Adam TC, Holbrook SJ, Schmitt RJ. Macroalgae size refuge from herbivory promotes alternative stable states on coral reefs. PLoS One, 13(9), e0202273 (2018)

43. B. D. Hassard, N. D. Kazarinoff, Y. H. Wan, Theory and application of Hopf bifurcation, Cambridge University Press, Cambridge, 1981.

44. Mumby, P.J., Hastings, A., Edwards, H.J.: Thresholds and the resilience of caribbean coral reefs. Nature 450(7166), 98-101 (2007)

45. Williams, D.E., Miller, M.W.: Coral disease outbreak: pattern, prevalence and transmission in acropora cervicornis. Marine Ecology Progress Series 301, 119-128 (2005)

46. Vollmer, S.V., Kline, D.I.: Natural disease resistance in threatened staghorn corals. Plos one 3(11), 3718 (2008)

47. Richardson, L.L.: Coral diseases: what is really known Trends in Ecology & Evolution 13(11), 438-443 (1998)

48. Kermack, W.O., McKendrick, A.G.: A contribution to the mathematical theory of epidemics. Proceedings of the royal society of london. Series A, Containing papers of a mathematical and physical character 115(772), 700-721 (1927)

49. Anderson, R.M., May, R.M.: Infectious diseases and population cycles of forest insects. Science 210(4470), 658-661 (1980)

50. Fisher, E.M., Fauth, J.E., Hallock, P., Woodley, C.M.: Lesion regeneration rates in reef-building corals montastraea spp. as indicators of colony condition. Ecology Progress Series, 339, 61-71 (2007)

51. MacDonald, M. Time delays in biological models, Springer, Heidelberg (1978)

52. Yang, X., Chen, L., Chen, J.: Permanence and positive periodic solution for the single-species nonautonomous delay diffusive models. Computers and mathematics with applications, 32(4), 109-116 (1996)

53. Dieudonne, J.: Foundations of Modern Analysis. Read Books Ltd (2011).

54. Freedman, H.I., Rao, V.S.H.: The trade-off between mutual interference and time lags in predator-prey systems. Bulletin of Mathematical Biology, 45(6), 991-1004 (1983)

APPENDIX A.

According to the Riesz representation theorem, there exists a function $\eta(\theta,\mu)$ of bounded variation for $\theta \in [-1,0]$ such that

$$L_\mu \psi = \int_{-1}^{0} d\eta(\theta,\mu)\psi(\theta), \qquad for \quad \psi \in \mathbf{C}. \tag{7.1}$$

In particular, we set

$$\eta(\theta,\mu) = (\tau_0^* + \mu)A\delta(\theta) - (\tau_0^* + \mu)B\delta(\theta+1), \tag{7.2}$$

with

$$\delta(\theta) = \begin{cases} 1, & \theta=0, \\ 0, & \theta\neq 0. \end{cases}$$

Now, for ψ in $\mathbf{C}^1([-1,0],\mathbf{R}_+^{\mathbf{3}})$, we define

$$A(\mu)\psi = \begin{cases} \frac{d\psi(\theta)}{d\theta} & \theta \in [-1,0), \\ \int_{-1}^{0} d\eta(\mu,s)\psi(s) & \theta = 0, \end{cases}$$

and

$$R(\mu)\psi = \begin{cases} 0, & \theta \in [-1,0), \\ F(\mu,\psi), & \theta = 0. \end{cases}$$

Then, the system (5.15) takes the form

$$\dot{z_t} = A(\mu)z_t + R(\mu)z_t, \tag{7.3}$$

where $z_t(\theta) = z_t(t+\theta)$ for $\theta \in [-1,0]$.

For any ϕ in $\mathbf{C}^1([0,1],(\mathbf{R}_+^{\mathbf{3}})^*)$, we define

$$A^*\phi(s) = \begin{cases} -\frac{d\phi(s)}{ds}, & s \in (0,1], \\ \int_{-1}^{0} d\eta^T(t,0)\phi(-t), & s = 0, \end{cases}$$

and a bilinear inner product of the form

$$\langle \phi(s), \psi(\theta)\rangle = \overline{\phi}(0)\psi(0) - \int_{-1}^{0}\int_{\alpha=0}^{\theta} \overline{\phi}(\alpha-\theta)d\eta(\theta)\psi(\alpha)d\alpha, \tag{7.4}$$

where $\eta(\theta) = \eta(\theta,0)$, $A(0)$ and A^* denote the adjoint operators. From the section (5.1), we know that $\pm i\delta_0\tau_0^*$ are characteristic values of $A(0)$, which are also characteristic values of A^*. Now, we find the characteristic function of $A(0)$ and A^* associated with $i\delta_0\tau_0^*$ and $-i\delta_0\tau_0^*$ respectively.

We assume that $q(\theta) = (1,u,w)^T e^{i\delta_0\tau_0^*\theta}$ and $q^*(s)$ are the characteristic functions of $A(0)$ and A^* associated with $i\delta_0\tau_0^*$ and $-i\delta_0\tau_0^*$, respectively. Thus we have $A(0)q(\theta) = i\delta_0\tau_0^* q(\theta)$. From the definition of $A(0)$, (7.1) and (7.2), it follows that

$$\tau_0^* \begin{pmatrix} l_{11} - l_{11}^{'}e^{-i\delta_0\tau_0^*} - i\delta_0 & l_{12} - l_{12}^{'}e^{-i\delta_0\tau_0^*} & l_{13} \\ l_{11}^{'}e^{-i\delta_0\tau_0^*} & l_{22} + l_{12}^{'}e^{-i\delta_0\tau_0^*} - i\delta_0 & 0 \\ l_{31} & l_{32} & l_{33} - i\delta_0 \end{pmatrix} q(\theta) = \begin{pmatrix} 0 \\ 0 \\ 0 \end{pmatrix}.$$

So, we obtain

$$\begin{aligned} q(\theta) &= (1,u,w)^T e^{i\delta_0\tau_0^*\theta} \\ &= \Big(1, -\frac{l_{11}^{'} e^{-i\delta_0\tau_0^*}}{l_{22}+l_{12}^{'}e^{-i\delta_0\tau_0^*}-i\delta_0}, -\frac{l_{31}(l_{22}+l_{12}^{'}e^{-i\delta_0\tau_0^*}-i\delta_0)-l_{32}l_{11}^{'}e^{-i\delta_0\tau_0^*}}{(l_{33}-i\delta_0)(l_{22}+l_{12}^{'}e^{-i\delta_0\tau_0^*}-i\delta_0)}\Big)^T e^{i\delta_0\tau_0^*\theta}. \end{aligned}$$

In a similar manner, one can obtain

$$\begin{aligned} q^*(s) &= D(1,u^*,w^*)^T e^{i\delta_0\tau_0^* s} \\ &= \Big(1, -\frac{(l_{33}+i\delta_0)(l_{11}-l_{11}^{'}e^{i\delta_0\tau_0^*}+i\delta_0)-l_{13}l_{31}}{(l_{33}+i\delta_0)l_{11}^{'}e^{i\delta_0\tau_0^*}}, -\frac{l_{13}}{(l_{33}+i\delta_0)}\Big)^T e^{i\delta_0\tau_0^* s}. \end{aligned}$$

We choose D with the property of $\langle q^*(s), q(\theta)\rangle = 1$, $\langle q^*(s), \overline{q}(\theta)\rangle = 0$. Then, we have

$$\begin{aligned} \langle q^*(s), q(\theta)\rangle &= \overline{D}(1,\overline{u^*},\overline{w^*})(1,u,w)^T \\ &\quad - \int_{-1}^{0}\int_{\alpha=0}^{\theta} \overline{D}(1,\overline{u^*},\overline{w^*}) e^{-i\delta_0\tau_0^*(\alpha-\theta)} d\eta(\theta)(1,u,w)^T e^{i\delta_0\tau_0^*\alpha} d\alpha \\ &= \overline{D}\left[1+\overline{u^*}u+\overline{w^*}w - \int_{-1}^{0}(1,\overline{u^*},\overline{w^*})\theta e^{i\delta_0\tau_0^*\theta} d\eta(\theta)(1,u,w)^T\right] \\ &= \overline{D}\left[1+\overline{u^*}u+\overline{w^*}w - \tau_0^*\{l_{11}^{'}(u^*-1)+l_{12}^{'}(w^*-1)u\}e^{-i\delta_0\tau_0^*}\right]. \end{aligned}$$

Thus, we get D as given by

$$D = \frac{1}{1+u^*\overline{u}+w^*\overline{w}-\tau_0^*\{l_{11}^{'}(\overline{u^*}-1)+l_{12}^{'}(\overline{w^*}-1)\overline{u}\}e^{i\delta_0\tau_0^*}}.$$

To describe the center manifold $\mathbf{C}_0$ near $\mu = 0$, we determine the components by using the same notation and procedure as developed by [43].
Letting z_t to be the solution of (5.15) for $\mu = 0$, we define

$$\mathrm{z}(t) = \langle q^*, z_t\rangle, \qquad W(t,\theta) = z_t(\theta) - 2Re\{\mathrm{z}(t)q(\theta)\}. \tag{7.5}$$

On the center manifold $\mathbf{C}_0$, we have

$$W(t,\theta) = W\Big(\mathrm{z}(t), \overline{\mathrm{z}}(t), \theta\Big),$$

where

$$W(\mathrm{z},\overline{\mathrm{z}},\theta) = W_{20}(\theta)\frac{\mathrm{z}^2}{2} + W_{11}(\theta)\mathrm{z}\overline{\mathrm{z}} + W_{02}(\theta)\frac{\overline{\mathrm{z}}^2}{2} + W_{30}(\theta)\frac{\mathrm{z}^3}{6} + \cdots,$$

z and $\overline{\mathrm{z}}$ are local coordinates for center manifold $\mathbf{C}_0$ in the direction of q^* and $\overline{q}^*$, respectively. Here, W is real for real values of z_t. For the value z_t in $\mathbf{C}_0$ of (5.15) with $\mu = 0$, we obtain

$$\begin{aligned} \dot{\mathrm{z}}(t) &= i\quad \delta_0\tau_0^*\mathrm{z} + \Big\langle \overline{q}^*(\theta), F\Big(0, W(\mathrm{z},\overline{\mathrm{z}},\theta) + 2Re\{\mathrm{z}q(\theta)\}\Big)\Big\rangle \\ &= i\delta_0\tau_0^*\mathrm{z} + \overline{q}^*(0)F\Big(0, W(\mathrm{z},\overline{\mathrm{z}},0) + 2Re\{\mathrm{z}q(0)\}\Big) \overset{\text{def}}{=} i\delta_0\tau_0^*\mathrm{z} + \overline{q}^*(0)F_0(\mathrm{z},\overline{\mathrm{z}}), \end{aligned}$$

which can be rewritten as

$$\dot{\mathrm{z}} = i\delta_0\tau_0^*\mathrm{z} + g(\mathrm{z},\overline{\mathrm{z}}),$$

with

$$g(\mathrm{z},\overline{\mathrm{z}}) = \overline{q}^*(0)F_0(\mathrm{z},\overline{\mathrm{z}}) = g_{20}\frac{\mathrm{z}^2}{2} + g_{11}\mathrm{z}\overline{\mathrm{z}} + g_{02}\frac{\overline{\mathrm{z}}^2}{2} + g_{21}\frac{\mathrm{z}^2\overline{\mathrm{z}}}{2} + \cdots. \tag{7.6}$$

Then, from (7.5), we have

$$\begin{aligned} z_t(\theta) &= (z_{1t}(\theta), z_{2t}(\theta), z_{3t}(\theta))^T = W(t,\theta) + 2Re\{\mathrm{z}(t)q(\theta)\} \\ &= W_{20}(\theta)\frac{\mathrm{z}^2}{2} + W_{11}(\theta)\mathrm{z}\overline{\mathrm{z}} + W_{02}(\theta)\frac{\overline{\mathrm{z}}^2}{2} + (1,u,w)^T e^{i\delta_0\tau_0^*\theta}\mathrm{z} + (1,\overline{u},\overline{w})^T e^{-i\delta_0\tau_0^*\theta}\overline{\mathrm{z}} \\ &\quad + O(|\ (\mathrm{z},\overline{\mathrm{z}})\ |^3). \end{aligned} \tag{7.7}$$

In consequence, from Eq. (7.6), we can get

$$g(\mathrm{z},\overline{\mathrm{z}}) = \overline{q}^*(0)F_0(\mathrm{z},\overline{\mathrm{z}}) = \overline{D}(1,\overline{u^*},\overline{w^*})\tau_0^* \begin{pmatrix} m_{11}z_{1t}^2(0) + m_{12}z_{2t}^2(0) + m_{13}z_{1t}(0)z_{2t}(0) + m_{14}z_{1t}(0)z_{3t}(0) + m_{15}z_{2t}(0)z_{3t}(0) \\ +m_{16}z_{1t}(-1)z_{2t}(-1) \\ m_{21}z_{1t}(-1)z_{2t}(-1) \\ m_{31}z_{3t}^2(0) + m_{32}z_{1t}(0)z_{3t}(0) + m_{33}z_{2t}(0)z_{3t}(0) \end{pmatrix}.$$

By direct calculation and comparing the coefficients with (7.6), we obtain

$$\begin{aligned} g_{20} &= 2\overline{D}\tau_0^*\Big[m_{11} + m_{12}u^2 + m_{13}u + m_{14}w + m_{15}uw + m_{16}ue^{-2i\delta_0\tau_0^*} \\ &\quad + \overline{u^*}m_{21}ue^{-2i\delta_0\tau_0^*} + \overline{w^*}\Big\{m_{31} + m_{32}w + m_{33}uw\Big\}\Big], \\ g_{11} &= 2\overline{D}\tau_0^*\Big[m_{11} + m_{12}|u|^2 + m_{13}Re\{u\} + m_{14}Re\{w\} + m_{15}Re\{u\overline{w}\} \\ &\quad + m_{16}Re\{u\} + \overline{u^*}m_{21}Re\{u\} + \overline{w^*}\Big\{m_{31} + m_{32}Re\{w\} + m_{33}Re\{u\overline{w}\}\Big\}\Big], \\ g_{02} &= 2\overline{D}\tau_0^*\Big[m_{11} + m_{12}\overline{u}^2 + m_{13}\overline{u} + m_{14}\overline{w} + m_{15}\overline{uw} + m_{16}\overline{u}e^{2i\delta_0\tau_0^*} \\ &\quad + \overline{u}^*m_{21}\overline{u}e^{2i\delta_0\tau_0^*} + \overline{w}^*\Big\{m_{31} + m_{32}\overline{w} + m_{33}\overline{uw}\Big\}\Big], \\ g_{21} &= \overline{D}\tau_0^*\Big[m_{11}\Big(2W_{20}^1(0) + 4W_{11}^1(0)\Big) + m_{12}\Big(2\overline{u}W_{20}^2(0) + 4uW_{11}^2(0)\Big) \\ &\quad + m_{13}\Big(W_{20}^2(0) + 2W_{11}^2(0) + \overline{u}W_{20}^1(0) + 2uW_{11}^1(0)\Big) \\ &\quad + m_{14}\Big(W_{20}^3(0) + 2W_{11}^3(0) + \overline{w}W_{20}^1(0) + 2wW_{11}^1(0)\Big) \\ &\quad + m_{15}\Big(\overline{u}W_{20}^3(0) + 2uW_{11}^3(0) + \overline{w}W_{20}^2(0) + 2wW_{11}^2(0)\Big) \\ &\quad + m_{16}\Big(2W_{20}^2(-1)e^{i\delta_0\tau_0^*} + 2W_{11}^2(-1)e^{-i\delta_0\tau_0^*} + \overline{u}W_{20}^1(-1)e^{i\delta_0\tau_0^*} + 2uW_{11}^1(-1)e^{-i\delta_0\tau_0^*}\Big) \\ &\quad + \overline{u}^*m_{21}\Big(2W_{20}^2(-1)e^{i\delta_0\tau_0^*} + 2W_{11}^2(-1)e^{-i\delta_0\tau_0^*} + \overline{u}W_{20}^1(-1)e^{i\delta_0\tau_0^*} + 2uW_{11}^1(-1)e^{-i\delta_0\tau_0^*}\Big) \\ &\quad + \overline{w}^*\Big\{m_{31}\Big(2W_{20}^1(0) + 4W_{11}^1(0)\Big) + m_{32}\Big(\overline{w}W_{20}^2(0) + 2W_{11}^3(0) + 2wW_{11}^1(0) + 2W_{20}^3(0)\Big) \\ &\quad + m_{33}\Big(\overline{u}W_{20}^3(0) + 2uW_{11}^3(0) + \overline{w}W_{20}^2(0) + 2wW_{11}^2(0))\Big)\Big\}\Big]. \end{aligned}$$

To compute the value of g_{21}, we need to calculate the magnitude for the terms $W_{20}^i(\theta)$ and $W_{11}^i(\theta)$ $(i = 1,2,3)$. From (7.3) and (7.5), we have

$$\begin{aligned} \dot{W} = \dot{z}_t - \dot{z}q - \dot{\overline{\mathrm{z}}}\,\overline{q} &= \begin{cases} AW - 2Re\{\overline{q}^*(0)F_0q(\theta)\}, & \theta \in [-1,0), \\ AW - 2Re\{\overline{q}^*(0)F_0q(\theta)\} + F_0, & \theta = 0, \end{cases} \\ &\overset{\text{def}}{=} AW + H(\mathrm{z},\overline{\mathrm{z}},\theta), \end{aligned} \tag{7.8}$$

where

$$H(\mathrm{z},\overline{\mathrm{z}},\theta) = H_{20}(\theta)\frac{\mathrm{z}^2}{2} + H_{11}(\theta)\mathrm{z}\overline{\mathrm{z}} + H_{02}(\theta)\frac{\overline{\mathrm{z}}^2}{2} + \cdots. \tag{7.9}$$

Expanding the above series explicitly and comparing the corresponding coefficients, we get

$$(A - i2\delta_0\tau_0^* I)W_{20}(\theta) = -H_{20}(\theta), \quad AW_{11}(\theta) = -H_{11}(\theta). \tag{7.10}$$

From (7.8), we have

$$H(z,\bar{z},\theta) = -\overline{q}^*(0)F_0q(\theta) - q^*(0)\overline{F}_0\overline{q}(\theta) = -gq(\theta) - \overline{g}\ \overline{q}(\theta)\ for\theta\ \in [-1,0). \tag{7.11}$$

Comparing the associated coefficients with (7.9) yields

$$H_{20}(\theta) = -g_{20}q(\theta) - \overline{g}_{02}\overline{q}(\theta), \tag{7.12}$$
$$H_{11}(\theta) = -g_{11}q(\theta) - \overline{g}_{11}\overline{q}(\theta). \tag{7.13}$$

From (7.10), (7.12), (7.13) and utilizing the definition of A we obtain

$$\dot{W}_{20}(\theta) = i2\delta_0\tau_0^* W_{20}(\theta) + g_{20}q(\theta) + \overline{g}_{02}\overline{q}(\theta), \tag{7.14}$$

$$\dot{W}_{11}(\theta) = g_{11}q(\theta) + \overline{g}_{11}\overline{q}(\theta). \tag{7.15}$$

Since $q(\theta) = (1,u,w)^T e^{i\delta_0\tau_0^*\theta}$, therefore we have

$$W_{20}(\theta) = \tfrac{ig_{20}}{\delta_0\tau_0^*}q(0)e^{i\delta_0\tau_0^*\theta} + \tfrac{i\overline{g}_{20}}{3\delta_0\tau_0^*}\overline{q}(0)e^{-i\delta_0\tau_0^*\theta} + E_1e^{i2\delta_0\tau_0^*\theta}, \tag{7.16}$$

and

$$W_{11}(\theta) = -\tfrac{ig_{11}}{\delta_0\tau_0^*}q(0)e^{i\delta_0\tau_0^*\theta} + \tfrac{i\overline{g}_{11}}{\delta_0\tau_0^*}\overline{q}(0)e^{-i\delta_0\tau_0^*\theta} + E_2, \tag{7.17}$$

where $E_1 = (E_1^{(1)}, E_1^{(2)}, E_1^{(3)})$, $E_2 = (E_2^{(1)}, E_2^{(2)}, E_2^{(3)}) \in \mathbf{R}^3$ are constant vectors.
From the definition of A and utilizing (7.10) with $\eta(\theta) = \eta(0,\theta)$, we get

$$\int_{-1}^{0} d\eta(\theta)W_{20}(\theta) = i2\delta_0\tau_0^* W_{20}(0) - H_{20}(0), \tag{7.18}$$

and

$$\int_{-1}^{0} d\eta(\theta)W_{11}(\theta) = -H_{11}(0). \tag{7.19}$$

From (7.10), we have

$$H_{20}(0) = -g_{02}q(0) - \overline{g}_{02}\overline{q}(0) + 2\tau_0^* \begin{pmatrix} m_{11} + m_{12}u^2 + m_{13}u + m_{14}w + m_{15}uw + m_{16}ue^{-2i\delta_0\tau_0^*} \\ m_{21}ue^{-2i\delta_0\tau_0^*} \\ m_{31} + m_{32}w + m_{33}uw \end{pmatrix} \tag{7.20}$$

and

$$H_{11}(0) = -g_{11}q(0) - \overline{g}_{11}\overline{q}(0) + 2\tau_0^* \begin{pmatrix} m_{11} + m_{12}|u|^2 + m_{13}Re\{u\} + m_{14}Re\{w\} + m_{15}Re\{u\overline{w}\} + m_{16}Re\{u\} \\ m_{21}Re\{u\} \\ m_{31} + m_{32}Re\{w\} + m_{33}Re\{u\overline{w}\} \end{pmatrix}. \tag{7.21}$$

Notice that

$$\Big(i\delta_0\tau_0^* I - \int_{-1}^{0} e^{i\delta_0\tau_0^*\theta}d\eta(\theta)\Big)q(0) = 0, \quad \Big(-i\delta_0\tau_0^* I - \int_{-1}^{0} e^{-i\delta_0\tau_0^*\theta}d\eta(\theta)\Big)\overline{q}(0) = 0.$$

Substituting (7.16) and (7.20) into (7.18), we get

$$\Big(i2\delta_0\tau_0^* I - \int_{-1}^{0} e^{i2\delta_0\tau_0^*\theta}d\eta(\theta)\Big)E_1 = 2\tau_0^* \begin{pmatrix} m_{11} + m_{12}u^2 + m_{13}u + m_{14}w + m_{15}uw + m_{16}ue^{-2i\delta_0\tau_0^*} \\ m_{21}ue^{-2i\delta_0\tau_0^*} \\ m_{31} + m_{32}w + m_{33}uw \end{pmatrix},$$

which implies that

$$\begin{pmatrix} i2\delta_0 - l_{11} + l_{11}^{'} e^{-i2\delta_0\tau_0^*} & -l_{12} + l_{12}^{'} e^{-i2\delta_0\tau_0^*} & -l_{13} \\ -l_{11}^{'} e^{-i2\delta_0\tau_0^*} & i2\delta_0 - l_{22} - l_{12}^{'} e^{-i2\delta_0\tau_0^*} & 0 \\ -l_{31} & -l_{32} & i2\delta_0 - l_{33} \end{pmatrix} E_1 = 2 \begin{pmatrix} m_{11} + m_{12}u^2 + m_{13}u + m_{14}w + \\ m_{15}uw + m_{16}ue^{-2i\delta_0\tau_0^*} \\ m_{21}ue^{-2i\delta_0\tau_0^*} \\ m_{31} + m_{32}w + m_{33}uw \end{pmatrix},$$

It then follows that

$$E_1 = (E_1^{(1)}, E_1^{(2)}, E_1^{(3)}) = (\frac{|\Delta_{11}|}{|\Delta_1|}, \frac{|\Delta_{12}|}{|\Delta_1|}, \frac{|\Delta_{13}|}{|\Delta_1|}), \tag{7.22}$$

where

$$\Delta_1 = \begin{pmatrix} i2\delta_0 - l_{11} + l_{11}^{'} e^{-i2\delta_0\tau_0^*} & -l_{12} + l_{12}^{'} e^{-i2\delta_0\tau_0^*} & -l_{13} \\ -l_{11}^{'} e^{-i2\delta_0\tau_0^*} & i2\delta_0 - l_{22} - l_{12}^{'} e^{-i2\delta_0\tau_0^*} & 0 \\ -l_{31} & -l_{32} & i2\delta_0 - l_{33} \end{pmatrix}$$

and Δ_{1j} is obtained from Δ_1 by replacing jth column in to $2(m_{11} + m_{12}u^2 + m_{13}u + m_{14}w + m_{15}uw + m_{16}ue^{-2i\delta_0\tau_0^*}, m_{21}ue^{-2i\delta_0\tau_0^*}, m_{31} + m_{32}w + m_{33}uw)^T$.
Similarly, substituting (7.17) and (7.21) into (7.19), we have

$$\left(\int_{-1}^{0} d\eta(\theta)\right) E_2 = 2\tau_0^* \begin{pmatrix} m_{11} + m_{12}|u|^2 + m_{13}Re\{u\} + m_{14}Re\{w\} + m_{15}Re\{u\overline{w}\} + m_{16}Re\{u\} \\ m_{21}Re\{u\} \\ m_{31} + m_{32}Re\{w\} + m_{33}Re\{u\overline{w}\} \end{pmatrix},$$

which implies that

$$\begin{pmatrix} l_{11} - l_{11}^{'} & l_{12} - l_{12}^{'} & l_{13} \\ -l_{11}^{'} & l_{22} - l_{12}^{'} & 0 \\ l_{31} & l_{32} & l_{33} \end{pmatrix} E_2 = 2 \begin{pmatrix} m_{11} + m_{12}|u|^2 + m_{13}Re\{u\} + m_{14}Re\{w\} + m_{15}Re\{u\overline{w}\} + m_{16}Re\{u\} \\ m_{21}Re\{u\} \\ m_{31} + m_{32}Re\{w\} + m_{33}Re\{u\overline{w}\} \end{pmatrix}, \text{ and}$$

hence

$$E_2 = (E_2^{(1)}, E_2^{(2)}, E_2^{(3)}) = (\frac{|\Delta_{21}|}{|\Delta_2|}, \frac{|\Delta_{22}|}{|\Delta_2|}, \frac{|\Delta_{23}|}{|\Delta_2|}), \tag{7.23}$$

where

$$\Delta_2 = \begin{pmatrix} l_{11} - l_{11}^{'} & l_{12} - l_{12}^{'} & l_{13} \\ -l_{11}^{'} & l_{22} - l_{12}^{'} & 0 \\ l_{31} & l_{32} & l_{33} \end{pmatrix}$$

and Δ_{2j} is obtained from Δ_2 by replacing jth column in to $2(m_{11} + m_{12}|u|^2 + m_{13}Re\{u\} + m_{14}Re\{w\} + m_{15}Re\{u\overline{w}\} + m_{16}Re\{u\}, m_{21}Re\{u\}, m_{31} + m_{32}Re\{w\} + m_{33}Re\{u\overline{w}\})^T$.
Based on the foregoing arguments, we find that

$$C_1(0) = \frac{i}{2\delta_0\tau_0^*}\left(g_{20}g_{11} - 2|g_{11}|^2 - \frac{1}{3}|g_{02}|^2\right) + \frac{1}{2}g_{21},$$

$$\mu_2 = -\frac{Re\{C_1(0)\}}{Re\{\acute{\mu}(\tau_0^*)\}},\ \beta_2 = 2Re\{C_1(0)\},\ \tau_2 = -\frac{Im\{C_1(0)\} + \mu_2 Im\{\acute{\mu}(\tau_0^*)\}}{\delta_0\tau_0^*}.$$

It is well known that μ_2 and β_2 determine the direction of Hopf-bifurcation and stability of bifurcating periodic solutions of the system (2.5) at $\tau = \tau_0^*$ on center manifold. From the above analysis, the proof of Theorem 5.2 is complete.

Santosh Biswas, *Buddhadev Ranjit*,
Centre for Mathematical Biology and Ecology
Department of Mathematics, Jadavpur University
188, Raja S.C. Mallik Road, Kolkata 700032, India.
E-mail address: sant.biswas@gmail.com, buddhamath.ranjit@gmail.com

and

Saddam Mollah,
Gargi Memorial Institute of Technology,
Baruipur, Kolkata 700144, India

E-mail address: saddam.mollah13@gmail.com

and

Joydev Chattopadhyay,
Agricultural and Ecological Research Unit,
Indian Statistical Institute, 203 B. T. Road, Kolkata 700108, India
E-mail address: joydev@isical.ac.in

and

Subhas Khajanchi,
Department of Mathematics,Presidency University
86/1 College Street, Kolkata 700073, India
E-mail address: subhas.maths@presiuniv.ac.in

and

Bashir Ahmad,
Nonlinear Analysis and Applied Mathematics (NAAM)-Research Group,
Department of Mathematics, Faculty of Science, King Abdulaziz University,
P.O. Box 80203, Jeddah 21589, Saudi Arabia
E-mail address: bashirahmad_qau@yahoo.com